AD-A167 186 BURSTS AND PRESSURE FLUCTUATIONS IN TURBULENT BOUNDARY 1/1
LAYERS(U) IMPERIAL COLL OF SCIENCE AND TECHNOLOGY
LONDON (ENGLAND) DEPT OF AERONAUTICS P BRADSHAW ET AL.
UNCLASSIFIED JAN 86 DAJA45-84-C-0049 F/G 20/4 NL

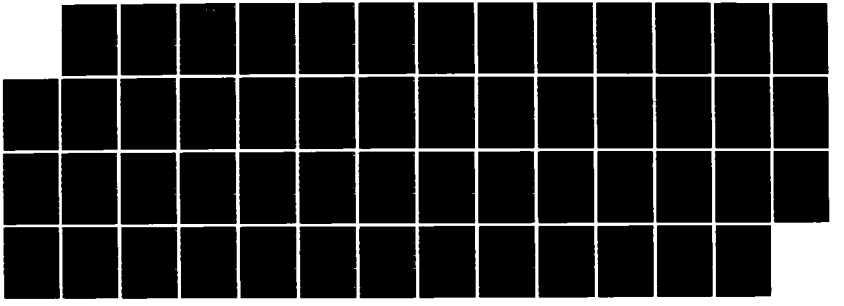

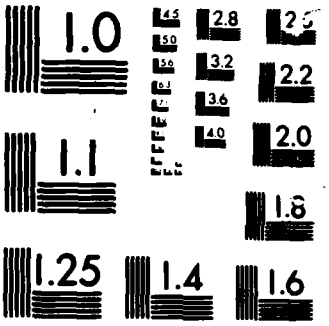
1.0
1.1
1.25
1.4
1.6
1.8
2.0
2.2
2.8
3.2
3.6
4.0
4.5
5.0
MICROCOPY
CHART

AD

BURSTS AND PRESSURE FLUCTUATIONS IN TURBULENT BOUNDARY LAYERS

Final Technical Report

by

P. Bradshaw and J.F. Morrison

January 1986

United States Army

EUROPEAN RESEARCH OFFICE OF THE U.S. ARMY

London England

CONTRACT NUMBER DAJA-45-84-C-0049

Department of Aeronautics

Imperial College, London SW7 2BY

Approved for Public Release; distribution unlimited

REPORT DOCUMENTATION PAGE

READ INSTRUCTIONS BEFORE COMPLETING FORM

1. REPORT NUMBER	2. GOVT ACCESSION NO. AD-A167886 / 3. RECIPIENT'S CATALOG NUMBER
4. TITLE (and Subtitle) Bursts and Pressure Fluctuations in Turbulent Boundary Layers	5. TYPE OF REPORT & PERIOD COVERED Final Technical Report Nov 84 - Nov 85
	6. PERFORMING ORG. REPORT NUMBER
7. AUTHOR(s) P. Bradshaw and J.F. Morrison	8. CONTRACT OR GRANT NUMBER(s) DAJA45-84-C-0049
9. PERFORMING ORGANIZATION NAME AND ADDRESS Department of Aeronautics Imperial College London SW7 2BY	10. PROGRAM ELEMENT, PROJECT, TASK AREA & WORK UNIT NUMBERS 61102A 1L161102BH57-06
11. CONTROLLING OFFICE NAME AND ADDRESS USARDSG-UK Box 65, FPO NY 09510-1500	12. REPORT DATE January 1986
	13. NUMBER OF PAGES 51
14. MONITORING AGENCY NAME & ADDRESS(if different from Controlling Office)	15. SECURITY CLASS. (of this report) Unclassified
	15a. DECLASSIFICATION/DOWNGRADING SCHEDULE

16. DISTRIBUTION STATEMENT (of this Report)

Approved for Public Release; distribution unlimited

17. DISTRIBUTION STATEMENT (of the abstract entered in Block 20, if different from Report)

18. SUPPLEMENTARY NOTES

19. KEY WORDS (Continue on reverse side if necessary and identify by block number)

Turbulent boundary layer, noise measurement, statistical analysis, surface roughness

20. ABSTRACT (Continue on reverse side if necessary and identify by block number)

This one year contract was an extension of DAJA37-81-C-0162 with the same title. In the present work, measurements of velocity and surface-pressure fluctuations have been made in a low speed constant pressure turbulent boundary layer well downstream of an extensive region of wall roughness. The turbulence near the wall was representative of a smooth-wall flow, while that in the outer layer was typical of the upper stream roygh-wall flow. Comparison with the previous measurements on an entirely smooth wall illustrates the

20. Contd.

relative contributions of the inner and outer layers to the surface pressure fluctuations. Further work has been done to compare the VITA conditional-sampling algorithm with more advanced algorithms.

Summary

This one year contract was an extension of DAJA37-81-C-0162 with the same title. In the present work, measurements of velocity and surface-pressure fluctuations were made in a low-speed constant-pressure turbulent boundary layer well downstream of an extensive region of wall roughness. The turbulence near the wall was representative of a smooth-wall flow, while that in the outer layer was typical of the upper stream rough-wall flow. Comparison with the previous measurements on an entirely smooth wall illustrates the relative contributions of the inner and outer layers to the surface pressure fluctuations. Further work has been done to compare the VITA conditional-sampling algorithm with more advanced algorithms.

Keywords:

Turbulent boundary layer, noise measurement, statistical analysis, surface roughness, V

Contents

Introduction

The contract DAJA37-81-C-0162 "Bursts and pressure fluctuations in turbulent boundary layers" was intended to study surface pressure fluctuations below turbulent boundary layers ~~both~~ were studied, in part, because of their intrinsic interest and because they can be regarded as ~~the~~ "footprints" of the passing turbulent eddies. The pressure fluctuations are formally described by a Poisson equation, implying that the pressure fluctuation at a given point is mathematically represented by the integral of a "source" term over the whole flow field, with a weighting inversely proportional to the distance of the source from the given point. In turbulent boundary layers, the high-frequency part of the wall pressure fluctuations is generated mainly within the inner layer - say, the first 20 ~~percent~~ of the boundary layer thickness - and the low-frequency part is generated mainly in the outer layer. In practice there is no sharp boundary between the inner and outer layers or between the two regions of the wall-pressure fluctuation spectrum. This limits the quantitative and qualitative usefulness of an experiment in a single boundary layer, and suggests that what is needed is a companion experiment in a flow in which the ratio of typical outer-layer turbulent intensity to inner-layer turbulent intensity is different from that in a simple constant-pressure smooth-wall flow. We briefly considered performing measurements in boundary layers in pressure gradients, or in boundary layers with the region of surface transpiration, but soon decided that the cleanest experiment for our purpose would be one in which the boundary layer initially developed over a rough surface, and then passed on to a smooth surface, both in zero pressure gradient. The

effect of the cessation of surface roughness spreads out in a "internal layer" or sub-boundary-layer, and we made our measurements at a distance downstream such that the whole of the inner layer ($y/\delta < 0.2$) had reverted to the equilibrium smooth-wall state, with a rapid increase of turbulence intensity outside the inner layer, the flow outside the "internal layer" being nominally unaffected by surface roughness change.

The change-of-roughness experiment seems to have been extremely successful. The change of velocity scale between the inner and outer layers shows up very clearly on the surface pressure fluctuation spectrum, and the changes in the velocity-fluctuation field in the inner layer provide additional useful information on the departures from universality of the structure, the so-called "inactive motion". (Briefly, non-universality of the turbulence structure in the inner layer is difficult to reconcile with the supposed universality of the logarithmic law used in so many calculation methods: but the present measurements should provide final conclusive data in support of the "inactive motion" concept, and incidentally provide searching test data for calculation methods.) The description of this work given below is based on the December 1984 - May 1985 periodic report, with some additions from the later data analysis: a paper for submission to Journal of Fluid Mechanics is in draft.

The other main activity during the year has been processing of data from the older smooth-wall experiment and the rough-to-smooth experiment. The object has been to use conditional sampling techniques to identify bursts of turbulence in the inner layer, which contribute a large part of the shear stress and the rms surface pressure fluctuation. The industry standard technique is the "variable interval time average" (VITA) algorithm of Blackwelder and Kaplan, which, essentially, recognises parts of a time-dependent signal in which the signal changes by more than a pre-chosen amount within a pre-chosen integration time. There has been a tendency in the literature to regard any event recognised by VITA as a turbulent

"burst", even when VITA has been applied simply to the u-component fluctuation, which is notorious for receiving contributions from all kinds of irrotational fluctuations and irrevelant turbulence as well as from the actual shear-stress-producing bursts.

We have produced an improved version of the VITA scheme in which the algorithm is applied to the uv signal, and detected events are classified according to the signs of u and v ("quadrant analysis"). We have also compared the VITA scheme with detection of excursions in the instantaneous temperature in the rough-to-smooth flow with a short region of the surface, near the change in surface roughness, slightly heated so that fluid in the outward-going eruptions further downstream would be "hot". This technique, which we have used in many other studies, is most simply thought of as a quantitative form of smoke-flow visualization.

Because this is a short-duration contract and because our interim reports have been fairly detailed, the present Final Report consists of three sections: (A) the two-month Periodic Report submitted in January 1985, (B) the six-month Periodic Report submitted in May 1985, and (C) a description of the conditional-sampling results, also in the form of a Periodic Report covering the final six months of the contract. Pages are numbered consecutively but are also marked "A", "B", or "C" to identify the sections listed above: figures are inserted at the end of each section.

Section (A) January 1985 2-month Periodic Report

Summary

This contract is an extension, to a fourth year, of DAJA37-81-C-0162 with the same title. The previous contract yielded extensive measurements of surface pressure fluctuations and related data on turbulent velocity fluctuations within the flow: the results are still being analysed, and publication has been delayed to incorporate the results of the present study. The object of the present work is to perturb the flow and thus the contributions to surface pressure fluctuations from different regions of the boundary layer. As well as the main Scientific Work statement, a selection of results is included for interest of U.S. Army scientific workers.

Scientific Work Statement

The first stage of the experiment outlined in the original extension proposal has been successfully completed and data analysis is well advanced. The work is intended to complement the studies reported under DAJA-37-81-C-0162, in which measurements were made of surface pressure fluctuations below a turbulent boundary layer in zero longitudinal mean pressure pressure gradient (a "flat plate" boundary layer). The high-frequency part of the surface pressure fluctuations arises from the small scale eddies near the surface, while the low-frequency part comes from the larger eddies in the outer part of the boundary layer. In reality the two contributions overlap and are difficult to distinguish, which complicates interpretation of results and development of prediction methods. The only way of proceeding is to set up an experiment in which the ratio of inner-layer to outer-layer contributions to the surface pressure fluctuation - i.e. the ratio of inner-layer to outer-layer turbulence intensity - is altered. The possibilities considered in the original proposal were

(i) apply a strong positive ("adverse") mean pressure gradient to the boundary layer, preferentially decelerating the flow

near the surface and consequently reducing the turbulence intensity there (the pressure fluctuations are not directly related to the mean pressure gradient)

(ii) initially develop the boundary layer over a rough wall, leading to high turbulence intensity throughout the layer, and then allow it to pass over a smooth wall so that the small-scale, fast-responding turbulence near the surface decays to an intensity typical of a smooth surface while the outer-layer turbulence remains unusually intense

(iii) initially develop the boundary layer over a surface with transpiration, leading to high turbulence intensity in the outer layer at least, and then pass to a smooth solid surface: the general effect is similar to (ii).

After some exploratory work we decided to adopt the second possibility, and we have carried out a complete set of measurements at one station downstream of a rough-to-smooth "transition" or "step", with supplementary measurements further upstream. The roughness is composed of an evenly distributed array of 1/2" cubes which is sufficiently three-dimensional for present purposes. The results show the desired separation of inner and outer layer contributions to p'_w in a very satisfactory way - the frequency spectrum of the pressure fluctuations, to be presented below, has a distinct "shelf" separating the low-frequency and high-frequency (outer and inner) contributions. The changes in surface pressure fluctuation statistics were unexpectedly large. We are still digesting the results and making the essential comparisons with the previous experiment on a conventional smooth-surface boundary layer.

Plans for Remainder of Period

Further measurements at different stations will be made to fill in the results, but the main effort will be on further analysis

of the data already obtained, in particular th evaluation of temperature-conditioned averages to explore the growth of the internal layer. We are confident of completing the work, and preparing papers for publication, by the end of the contract period.

Results

Figure 1 shows the test rig. As in the main contract, measurements have been made mainly in the boundary layer on the floor of the Department's 3ft x 3ft low speed wind tunnel. A spanwise line source of heat was placed immediately downstream of the roughness so that the new "internal" surface layer which grows from the end of the rough region can be distinguished from the rest of the flow: this temperature tagging technique is the same as that used in the main contract for distinguishing turbulent and non-turbulent fluid in the outer part of the boundary layer.

Figure 2 shows the shear stress profile measured at 1495 mm downstream of the end of the roughness. The outer part of the profile corresponds to the highly-turbulent rough-wall boundary layer, while the inner part has relaxed back - coincidentally - to very nearly the surface shear stress expected on a totally-smooth surface at the same local Reynolds number.

Figure 3 shows the mean velocity profile: briefly, the outer part of the profile as plotted on semi-logarithmic axes corresponds to the profile expected for the rough-wall boundary layer, while the inner part shows the law of the wall appropriate to the local smooth surface flow. Roughness decreases the flow speed near the surface, which is - indirectly - why the velocity in the central region falls below the extrapolated "law of the wall". This dip in the law of the wall occurs in several different kinds of perturbed boundary layer, and there is usually a quite simple explanation so that it need not be regarded as evidence of severe anomaly.

Figure 4 shows the pressure fluctuation frequency spectrum, of which the low-frequency part corresponds to the outer-layer eddies generated on the rough wall, while the high-frequency part depends on the small eddies near the surface, generated locally over the smooth wall. The crossed line shows the spectrum measured on a wholly-smooth wall, on corresponding scales. A simple dimensional analysis shows that the wave number spectrum should have a k^{-1} region with a coefficient which is a universal multiple of τ_w^2: a similar but less rigorous argument applies to the frequency spectrum. In the smooth wall measurements, the "universal multiple" was found to be $7.2*10^{-8}$, and the same value gives a good fit to the high-frequency part of the spectrum in the rough-to-smooth case, as seen from the good agreement of the full and dotted lines over the k^{-1} region and beyond.The k^{-1}region contributed by the eddies generated in the "law of the wall" region, $y/\delta < 0.2$ say, of the rough wall boundary layer would have an intercept roughly 8 times as large and of course cover a lower region of wave number: this k^{-1}line is not reached, because the inner layer of the rough wall boundary layer is absorbed by the internal layer (plus the disturbance created at the blunt base of the last row of roughness elements). In general, however, the experiment has succeeded rather well in highlighting the separate contributions of the rough wall boundary layer and the new internal layer formed over the smooth part of the wall.

Figure 5 shows a dimensionless parameter of the velocity fluctuation field. The decrease in the shear stress parameter near the surface, compared with smooth wall value, is caused by pressure fluctuations generated by the outer-layer ("rough wall") eddies, which induce tangential (u and w) velocity fluctuations near the surface but cannot generate significant vertical (v-component) fluctuations because of the constraint of the solid wall. As a result this induced motion does not contribute to the shear stress $-\overline{uv}$, and is called "inactive". Exactly the same argument can be applied to a smooth wall and explains the small y-dependence of the shear stress parameters for the smooth wall case: the large difference between the smooth wall and the roughness step demonstrates the largeness of the inactive motion in the latter case.

Figure 6 is a reproduction from Bradshaw (1967) in which wall pressure-velocity correlation measurements were made in a strong adverse pressure gradient. The large increase in the u-velocity correlation relative to the "flat plate" measurements near the wall is repeated in the present data shown by the crossed symbols and occurs for the same reasons as described above.

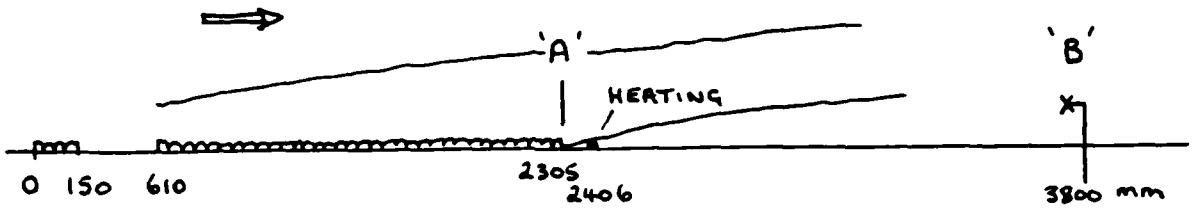

	STEP 1495 A	STEP 1495 B	Smooth
u_τ	1.77	1.05 ms^{-1}	1.09 ms^{-1}
u_e	33.5	33.5 ms^{-1}	32.8 ms^{-1}
δ_{995}	100.6	119.0 mm	68.2 mm
c_f	.00555	0.00196	0.00222
δ^*	19.38	18.65 mm	8.93 mm
θ	12.8	14.10 mm	6.93 mm
H	1.51	1.32	1.29
Re_θ	2.7_{10^4}	$3._{10^4}$	1.45_{10^4}

STEP 1495 (velocity measurements with τ_w and p_w sensors)

Rpp

Rpu Rpv Rpuv traverse with spanwise displacements.
Conventional 'on-line' statistics up to 4th order.
u, v, θ traverse
4 x-wire rake

STEP 1340 u, v, θ traverse

Fig.A1 Data Summary

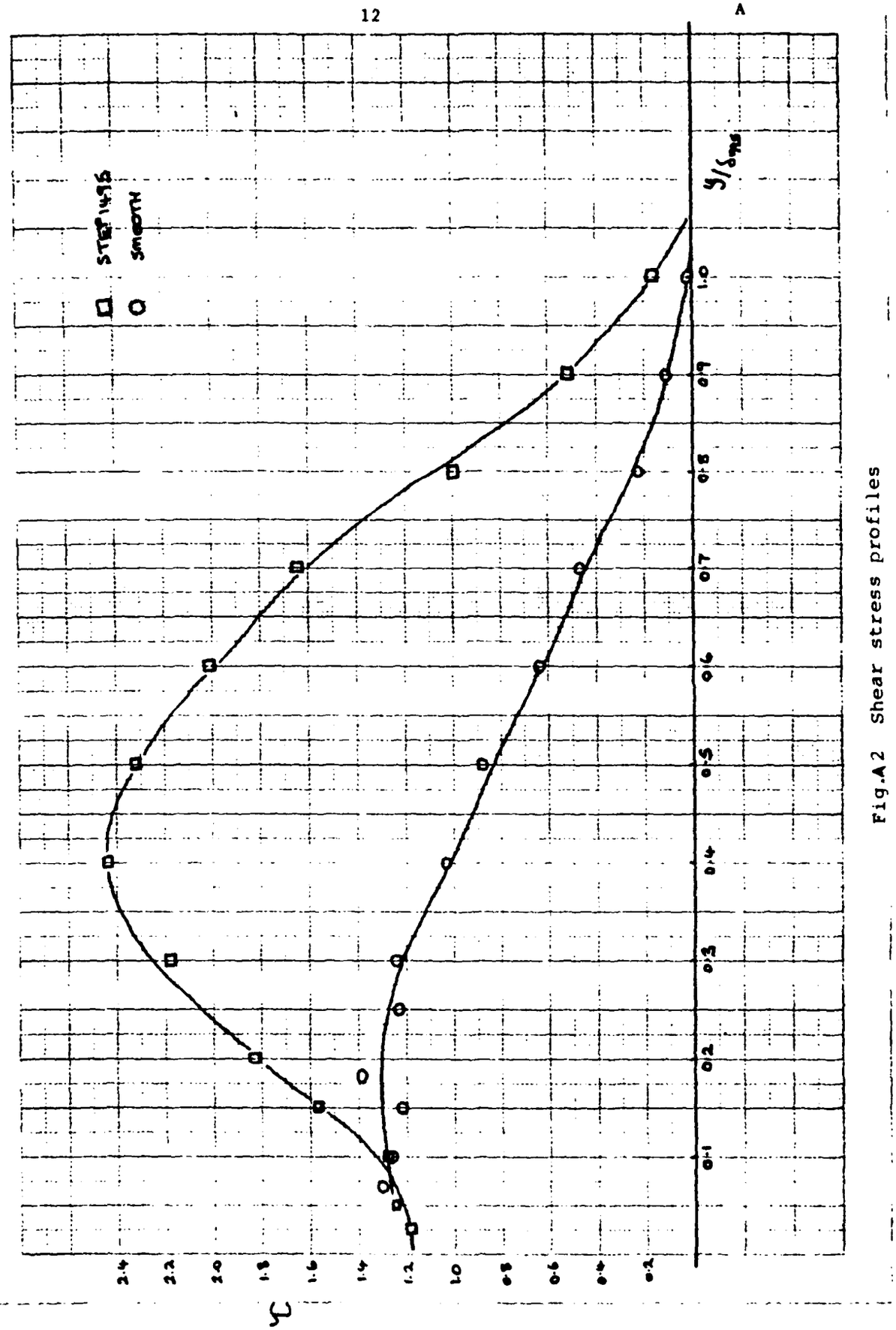

Fig.A2 Shear stress profiles

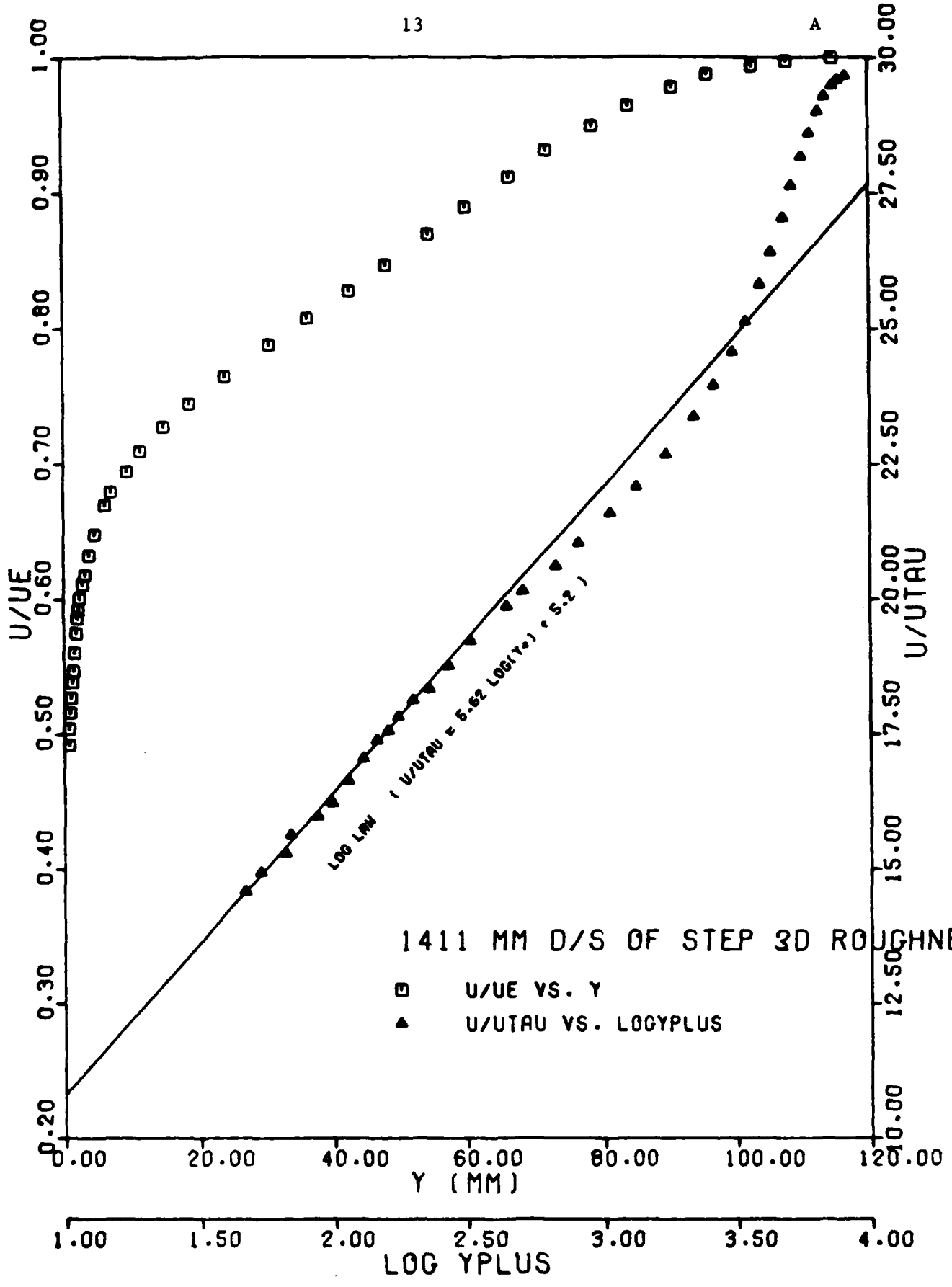

Fig.A3 Mean velocity profile and Clauser plot

$$\frac{\phi}{\rho^2 u_{\tau,B}^3 \nu} \quad \text{vs.} \quad \frac{\omega \nu}{u_{\tau,B}^2}$$

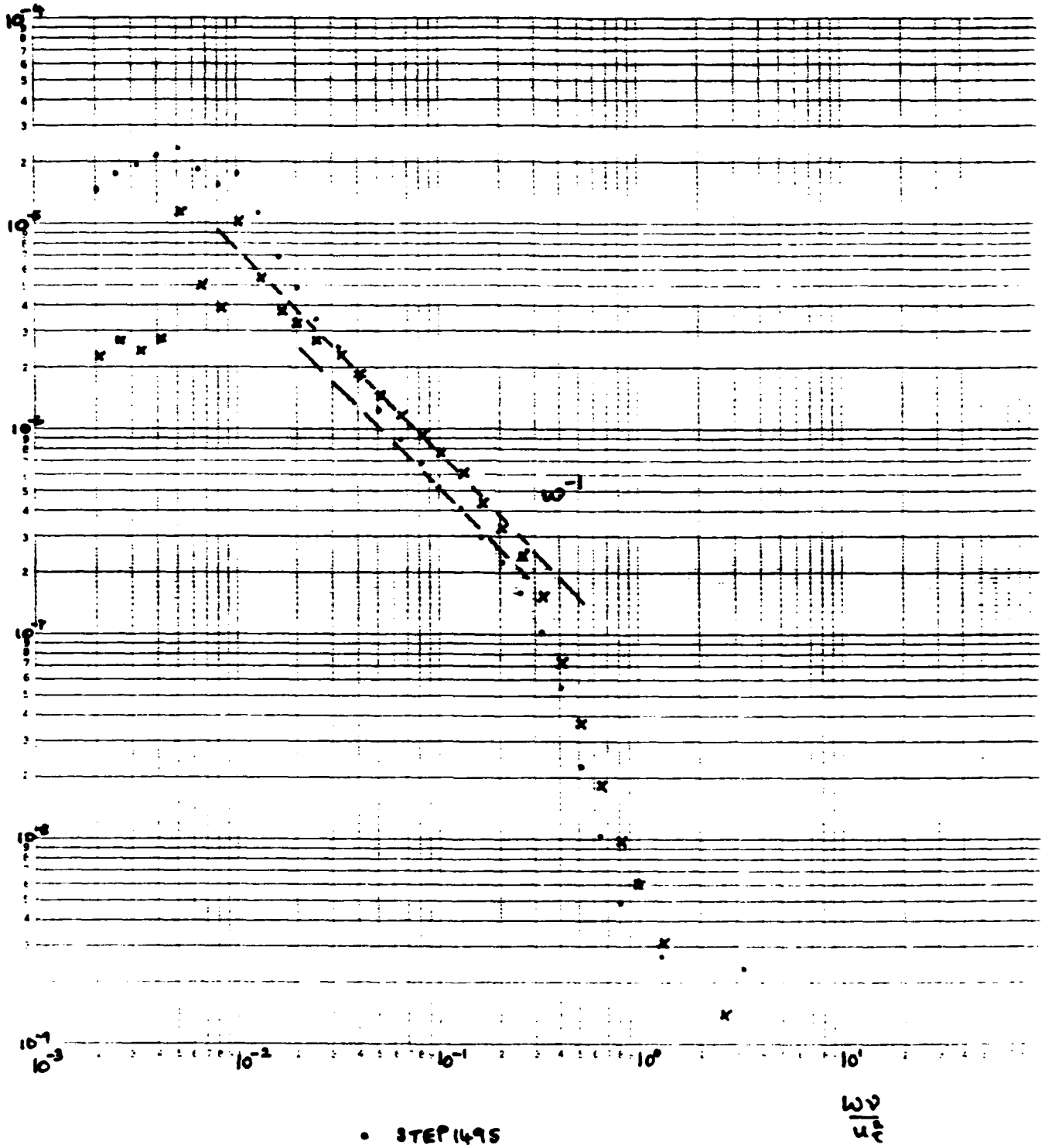

Chartwell Graph Data Ref. 8988 Log 5 Cycles x 5 Cycles

Fig. A4. Wall pressure spectra.

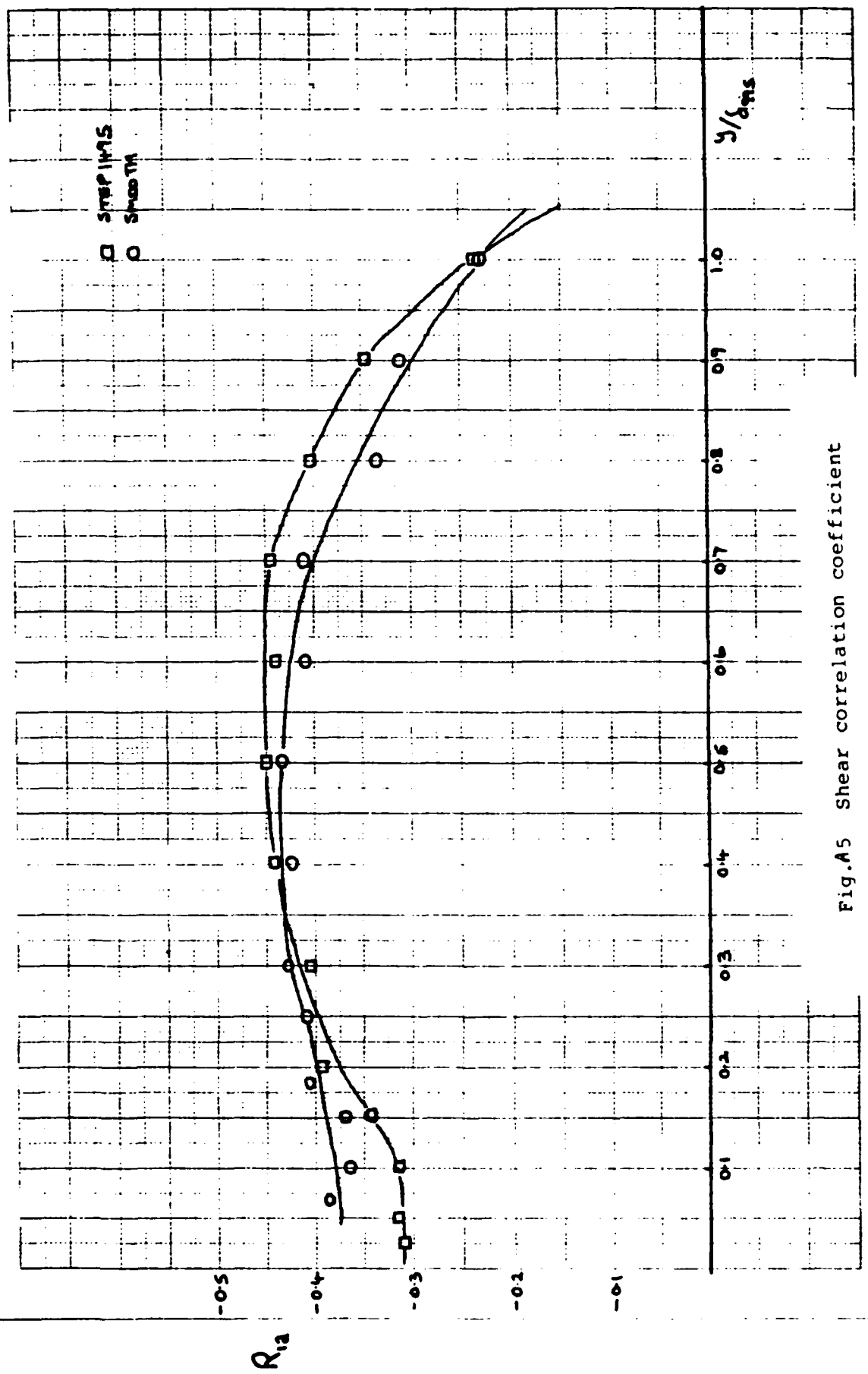

Fig.A5 Shear correlation coefficient

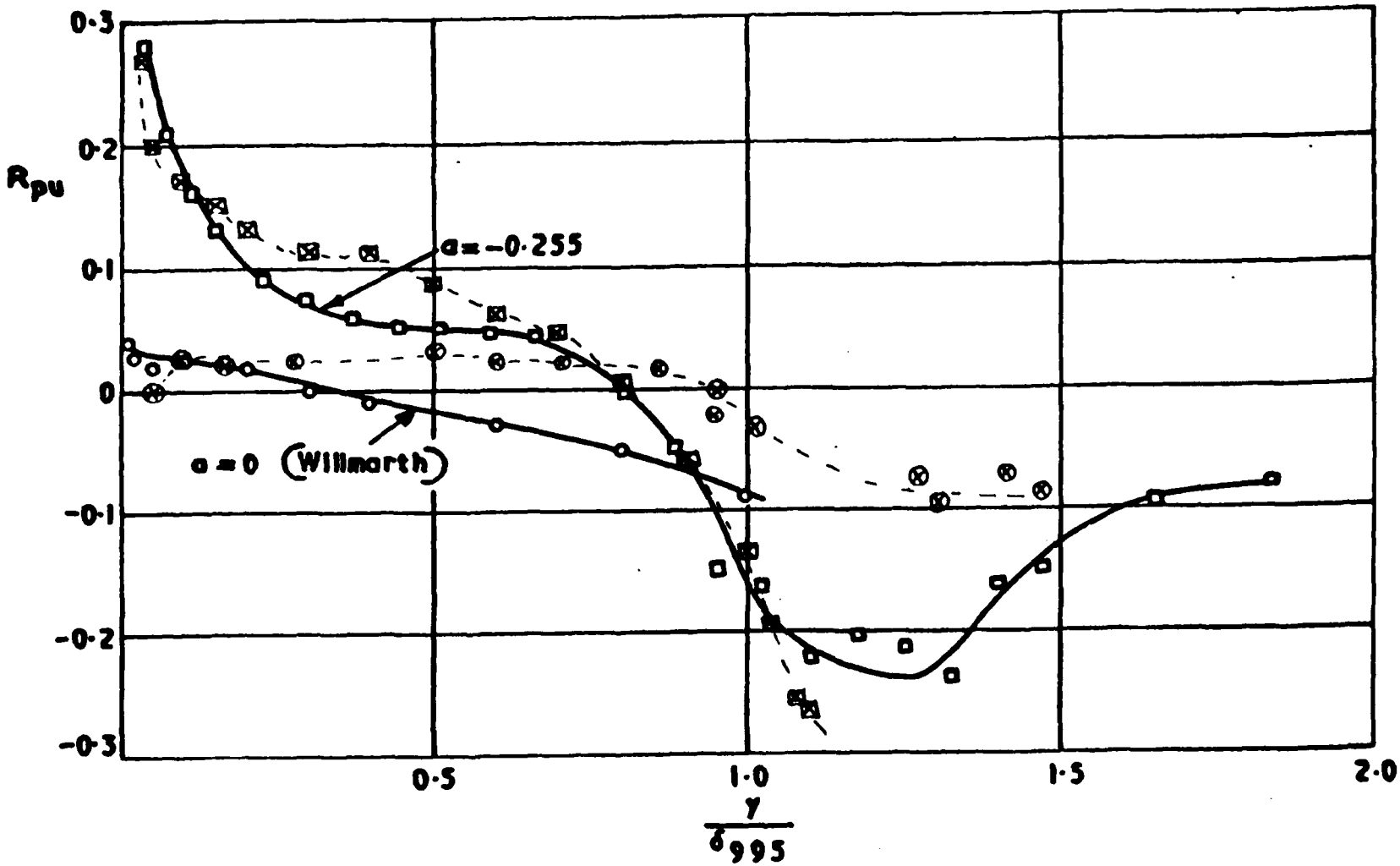

FIG 6. **Coefficient of correlation between the u component at height y and the pressure at the surface**

A

Section (B) May 1985 6-month Periodic Report

Summary

Analysis of the results acquired in the first stage of the experimental work has continued. The motivation for the experiment was described in the first periodic report, December 1984 - January 1985, which is Section A of the present Final Report. Comparisons of measurements in a boundary layer downstream of a region of large surface roughness with similar measurements on a wholly-smooth surface have proved extremely illuminating. Some analysis has also been done on measurements, taken under one of the Principal Investigator's other grants, in a boundary layer on a surface that was slightly heated after an initial adiabatic "starting length". The work is on schedule, and although some further measurements will be made most of the time will be spent on further analysis of the data bank already acquired.

Scientific Work Statement

The work statement presented in the December 1984 - January 1985 report is still qualitatively valid (see Section A). Continued analysis has confirmed the usefulness of comparisons between our previous measurements of turbulence and surface pressure fluctuations in a conventional boundary layer with the more recent experiment on the partly-rough plate shown in figure 1 of Section A. (In the latter case, measurements are actually made on the smooth part of the plate, in a boundary layer that started life on the rough part upstream.) We now have extensive space-time correlations between the surface pressure fluctuation and the velocity fluctuation field in the inner and outer parts of the boundary layer. The main object of the experiment is to distinguish the contributions to the surface pressure fluctuation from the inner-layer and outer-layer turbulence: the effect of upstream surface roughness is to increase the intensity of the outer-layer turbulence compared to that in the inner-layer which is dominated by local surface conditions. Pressure fluctuations generated in the outer layer perturb the velocity fluctuation field in

the inner layer by what may be described as "Bernoulli effect", as well as affecting the surface pressure fluctuations themselves, and our results help to quantify this phenomenon as well.

Our data analysis uses the statistical tools first applied to analogue processing of pressure fluctuation measurement one or two decades ago, combined with more modern, essentially digital, techniques such as conditional sampling. We are currently using data acquired by another investigator in a partially-heated boundary layer, using the instantaneous temperature of the flow as the equivalent of concentration of smoke or dye released at the surface, thus enabling outgoing eruptions ("bursts") to be positively identified. Our experiences with the VITA Variable Interval Time Averaging scheme have shown that it is somewhat limited in application and reliability. Therefore we have tried and tested a modified version in the partially-heated flow and are now using this for comparison with the analysis of other workers' experimental data and large eddy simulations.

As in previous reports, we are attaching a selection of results for the interest of other US Army scientific workers.

Plans for remainder of period

As well as continuing statistical analysis of existing data, in conjunction with SERC-supported post-processing of the Moin and Kim large eddy simulation data for a turbulent channel, in which pressure fluctuation data are of course available within the flow, we shall do further wind tunnel experiments to fill in gaps in the present data. We have some suspicions about the accuracy of some of our surface shear stress fluctuation data, because data taken by one of our collaborators appear to suffer severely from interference from the "rake" supporting the hot wire probes: our own probes produced much less interference, but some repeat work is indicated. Shortly, we shall begin to draft journal papers describing both stages of the work, the smooth-surface measurements made under contract

DAJA37-81-C-0162 having been held over until comparisons could be made with the partly-rough surface data.

Results

Figures A1 to A4 of Section A outline the behaviour of the boundary layer on the partly-rough surface. In particular, figure A2 shows shear stress at the main measurement station compared with smooth-wall results (the general trends of turbulence-intensity data are similar). It can be seen that the shear stress at the wall has fallen to approximately the smooth-surface value, whereas the shear stress and turbulence intensity in the longer-lived outer-layer eddies are much larger than for a wholly-smooth surface. Figure A4 shows that although the higher-frequency part of the wall pressure spectrum (i.e. the contributions from the inner layer) scales on local properties in the same way as on a smooth surface, there is a pronounced peak in the low-frequency region, corresponding to pressure fluctuations generated by the intense outer-layer turbulence in the rough-to-smooth flow. The new statistical results described below are mainly intended to elaborate on these comparisons.

Calculations of the mean velocity and shear stress have been made by the Bradshaw-Ferriss-Atwell method, partly because it provides helpful streamwise interpolations between the measurement stations and partly because the data may be useful in further refinement of the method. Some results are shown in figure B1.

Figure B2 shows space-time correlations of surface pressure fluctuations, for smooth and rough-to-smooth surfaces. Correlations with zero spatial separations Fourier-transform into the spectra shown in figure A4. Deduction of the convection velocity of pressure fluctuations of given wave number from the space-time correlations gives a semi-quantitative indication of the origin of pressure fluctuations of given wave number - namely, the distance above the

surface at which the convection velocity of the velocity-fluctuation pattern coincides with that of the surface pressure fluctuation at the same wave number. This work is still in progress.

Figure B3 shows pressure-velocity correlations, between the surface pressure fluctuation p_w and u, v or uv at a given distance above the surface, for a range of time delays. Here, the differences between smooth-surface and rough-to-smooth surface results is spectacularly large, particularly for the correlation coefficient of p_w and u, R_{pu}. The reason is that on the smooth surface with its fairly low turbulence intensity in the outer layer, R_{pu} for small y is genuinely a correlation between the surface pressure fluctuation and the velocity fluctuations that produce it, whereas the high intensity turbulence in the outer layer of the rough-to-smooth boundary layer effect both the surface pressure fluctuation and the inner-layer velocity fluctuation, leading to a large correlation between the two. It is noteworthy that the change in correlation shape is much more noticeable for R_{pu} than for R_{pv}. This agrees with the usual notions of "inactive motion", the continuity equation implying that large-scale fluctuations generated in the outer layer necessarily have small v-component velocity fluctuations close to the surface, so that the changes in R_{pv} are comparatively small (note the change in vertical scaling). R_{puv} however, is very much the same shape, although smaller. R_{pw} correlations have not been measured, but would be expected to show similar behaviour to R_{pu}. Figure B4 shows velocity fluctuation spectra scaled on inner-layer variables, which agree well with the 1967 results of Bradshaw. So far, we have measurements at only two y positions within the semi-logarithmic region of the rough-to-smooth flow, because, as figure A3 shows, that region is rather thin. Figure B5 shows correlations between the surface shear stress (deduced from the u component velocity fluctuation in the viscous sub-layer) and velocity fluctuations. Naturally, the correlation between τ_w' and u near the surface is large, and the two sets for smooth and rough-to-smooth surfaces are similar both in shape and size. The major difference is that $R_{\tau u}$ peaks at a smaller negative time delay. As mentioned above, we have some suspicions about the

quantitative accuracy of our surface shear stress fluctuation measurements, but the qualitative appearance of the data presented here can be relied on.

Finally a few sample measurements of temperature velocity correlations are included in figure 6. The wholly-smooth data were derived from another worker's tape recordings of fluctuations in a boundary layer slightly heated by a wire on the surface roughly half way down the working section. These data extend the comparison of the wholly-smooth and rough-to-smooth layers and are a prerequisite to the above-mentioned conditional sampling of wall pressure fluctuations. Temperature-conditioned averages of the rough-to-smooth data play an important part in elucidating the growth of the new internal layer. We do not at present propose surface-pressure fluctuation measurements in a partly-heated flow, because of the spurious temperature response of our pressure transducers.

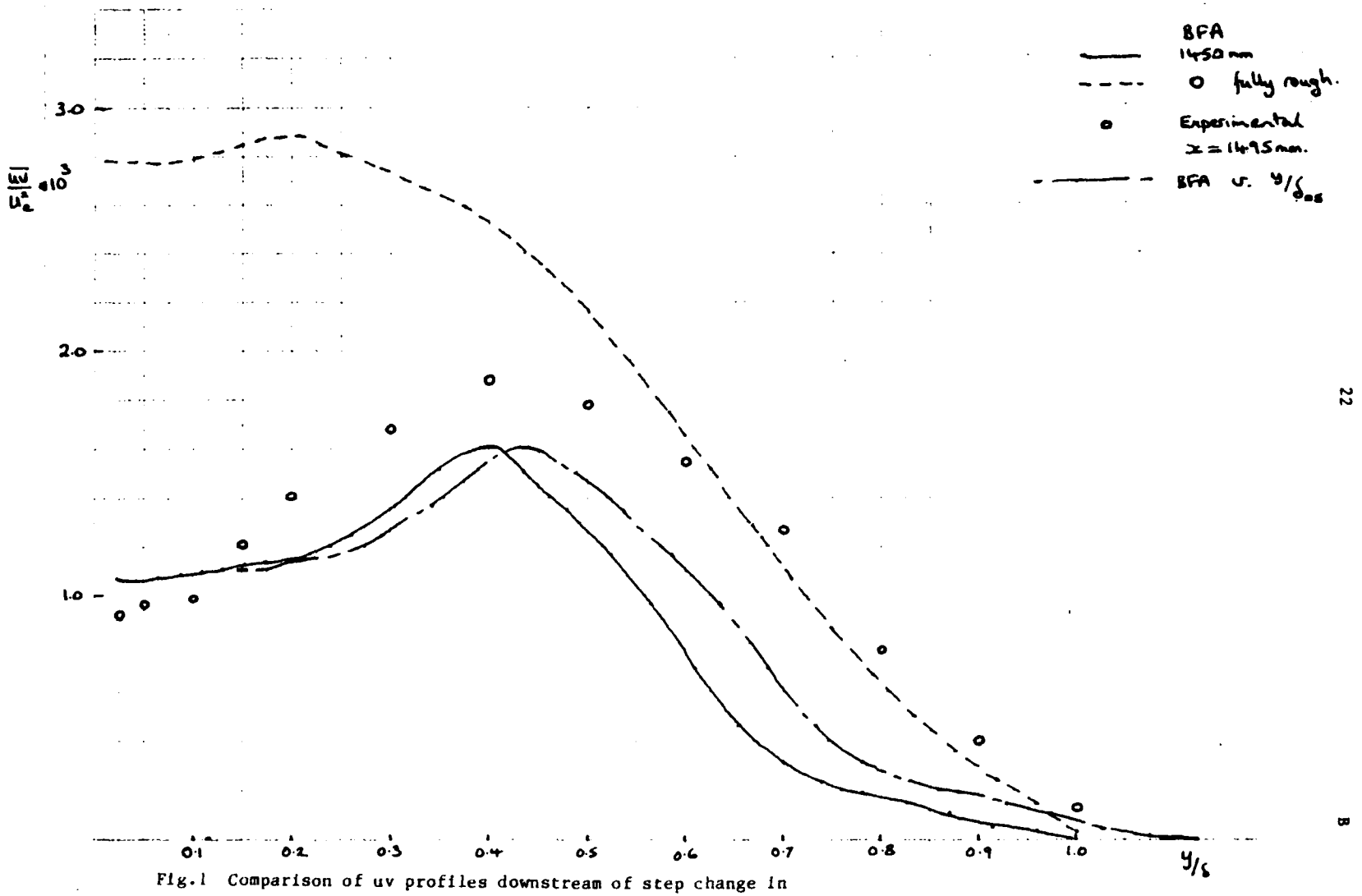

Fig.1 Comparison of uv profiles downstream of step change in roughness.

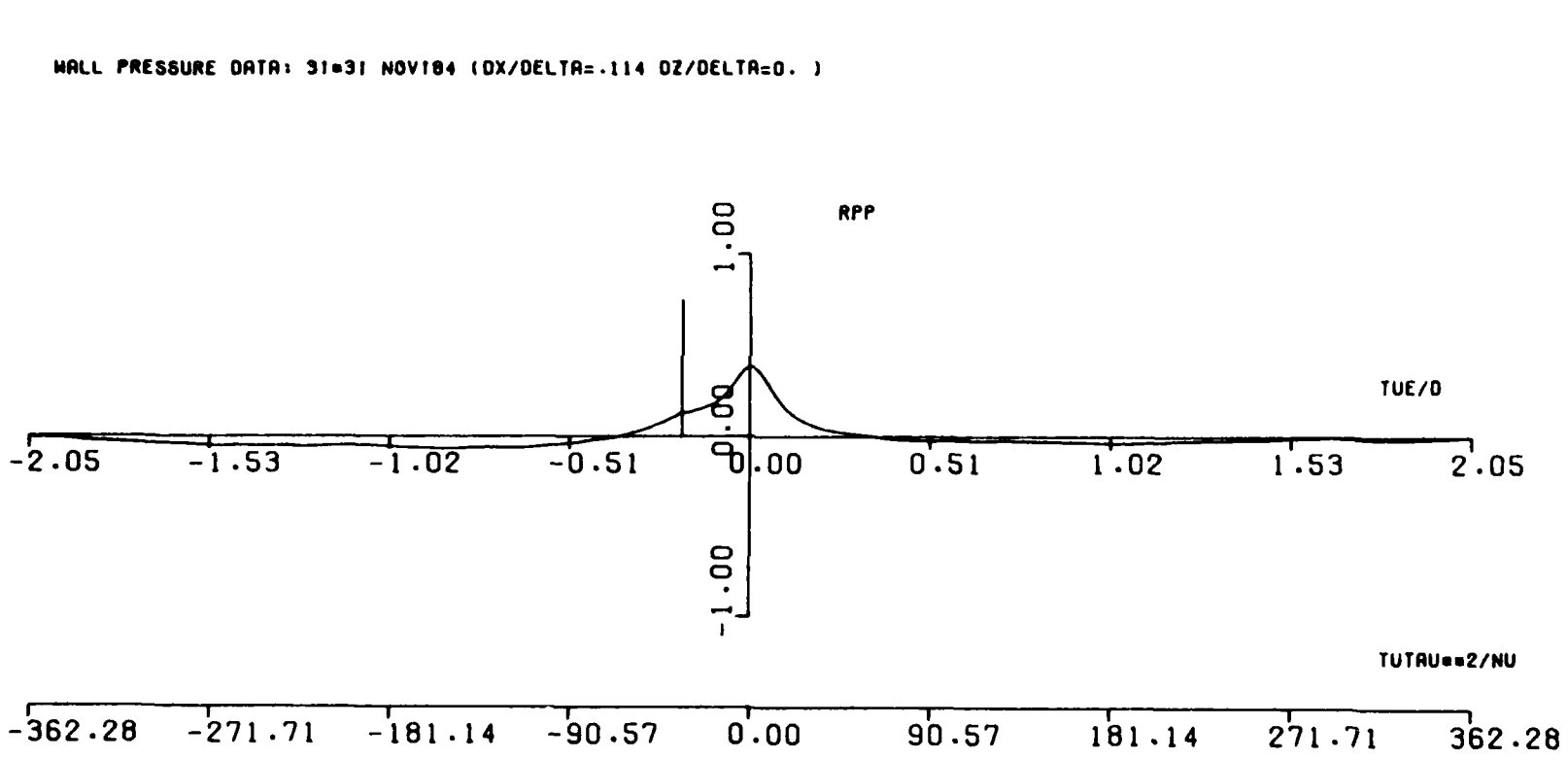

Fig.2 Pressure space-time correlations:

2(a) smooth $\Lambda x/\delta$ = .114

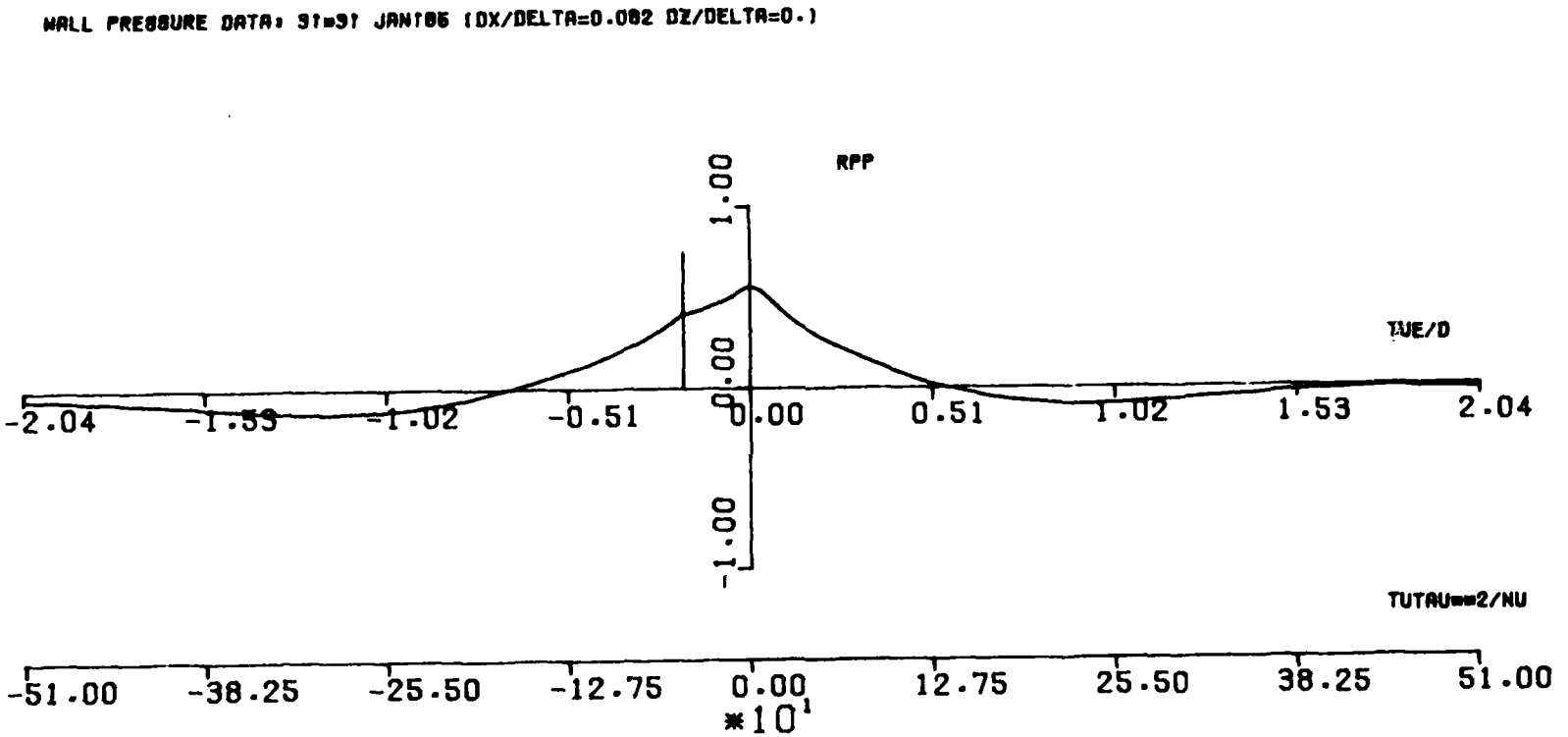

2(b) step $\Delta x/\delta$ = .082

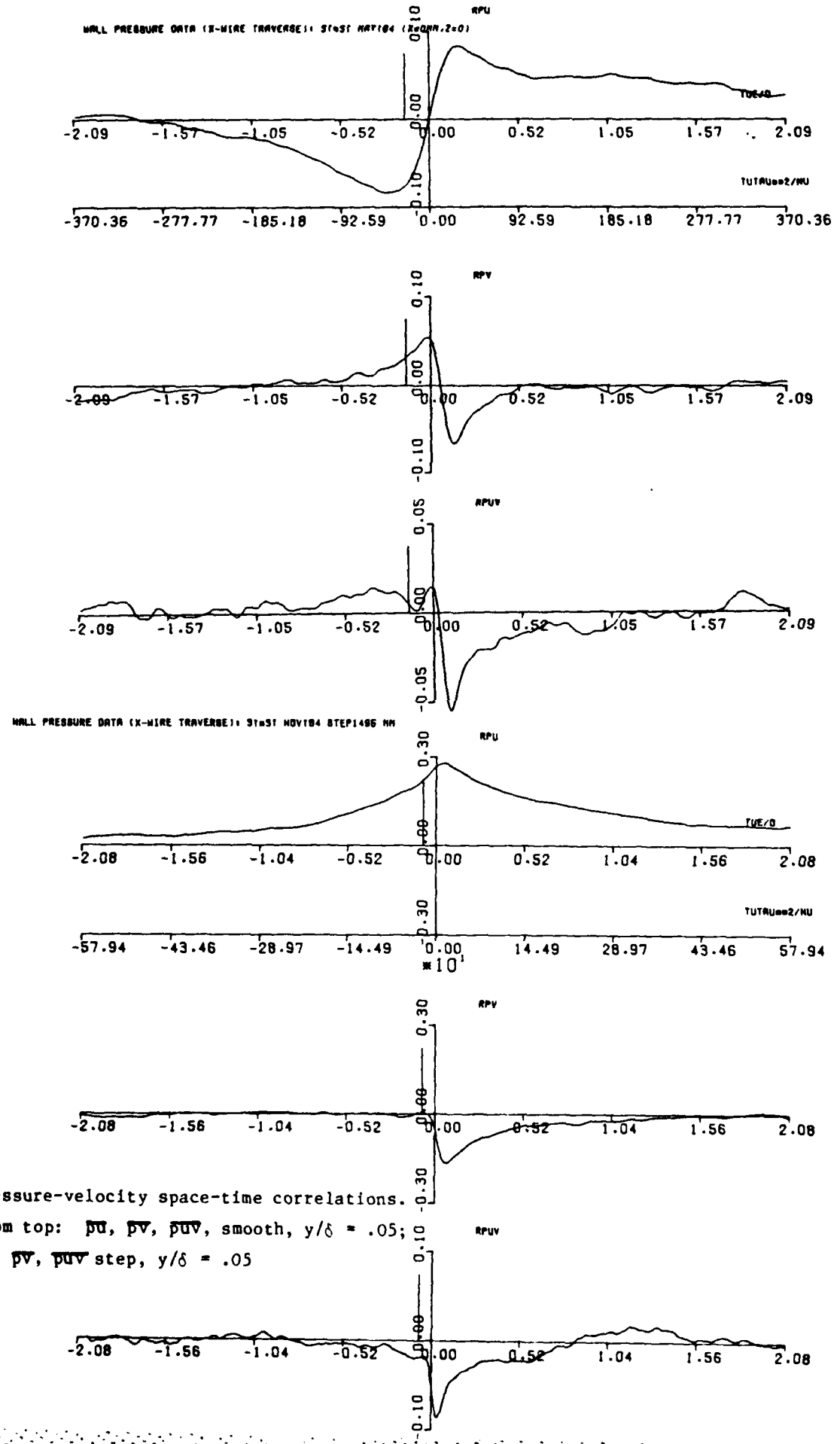

Fig.3

Pressure-velocity space-time correlations.
From top: $\overline{pu}$, $\overline{pv}$, $\overline{puv}$, smooth, y/δ = .05;
$\overline{pu}$, $\overline{pv}$, $\overline{puv}$ step, y/δ = .05

(ii)

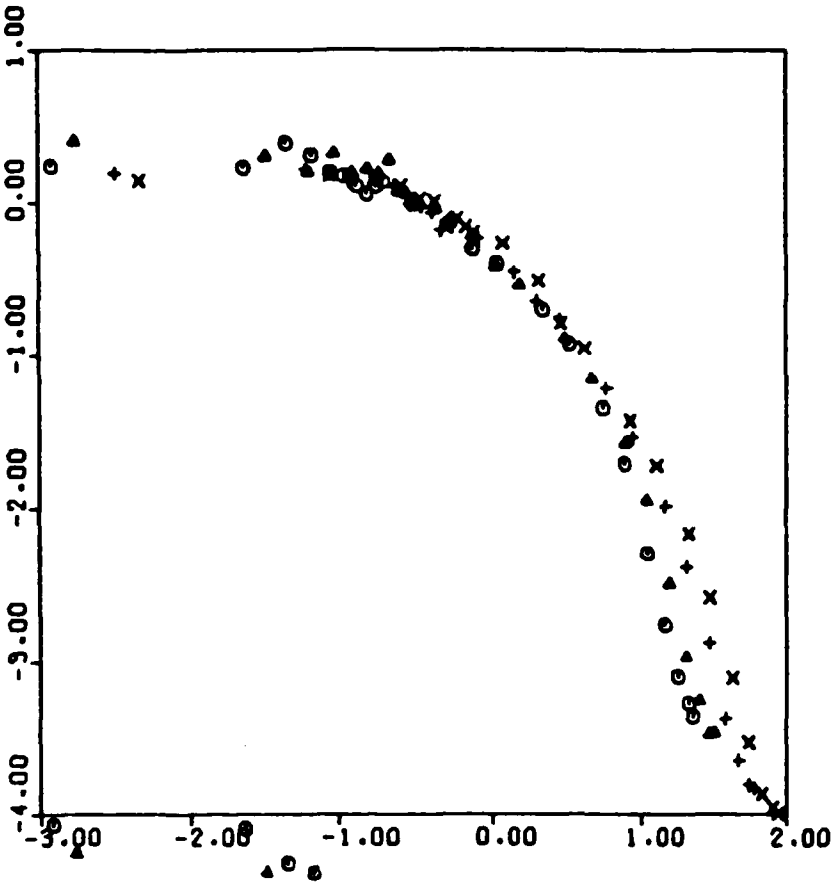

(i)

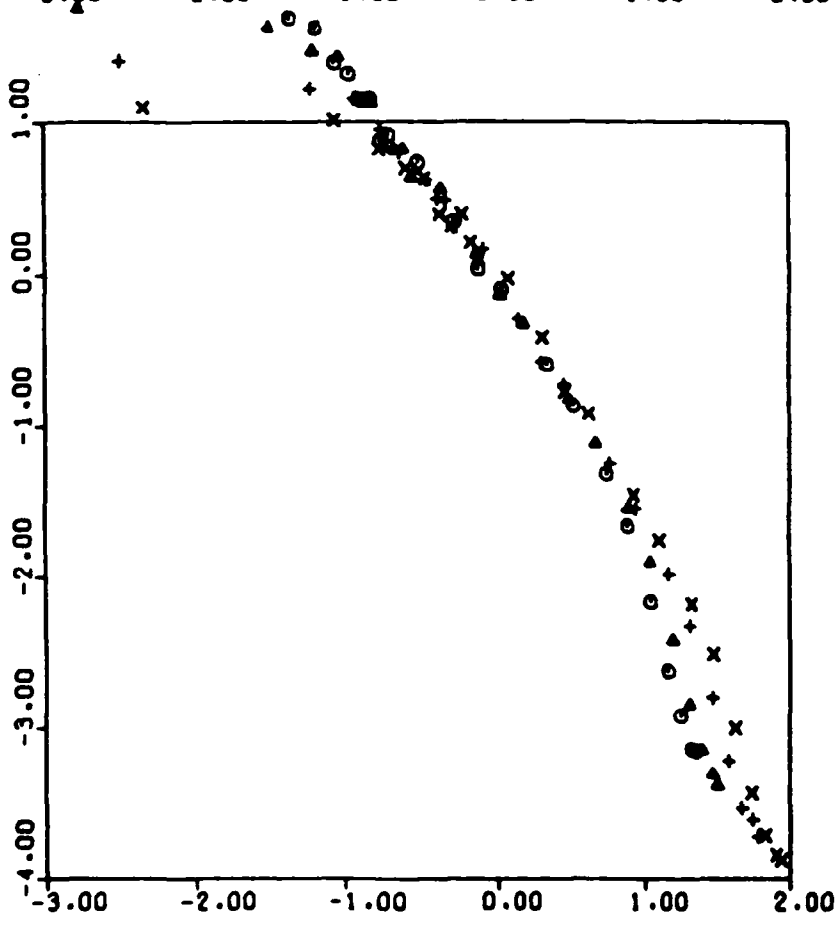

4(b) (i) ϕ_{uu} (ii) ϕ_{vv} rough-to-smooth

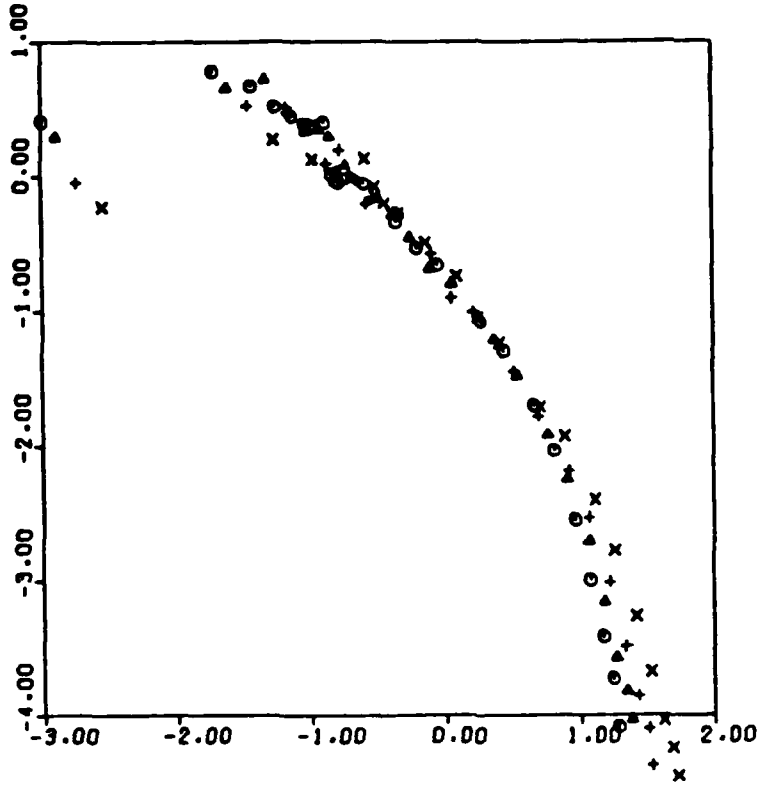

4(c) ϕ_{uv} smooth

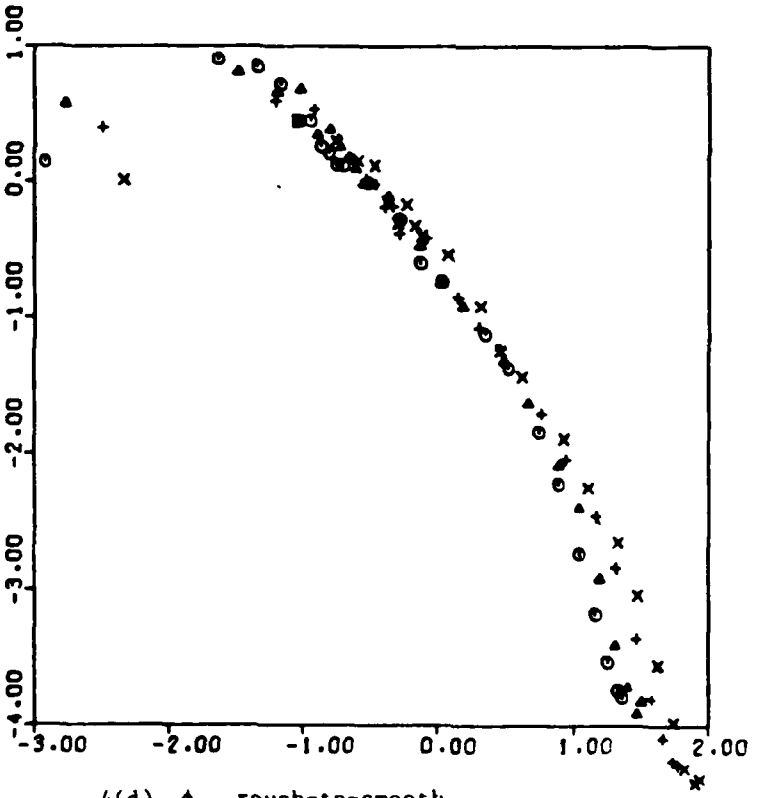

4(d) ϕ_{uv} rough-to-smooth

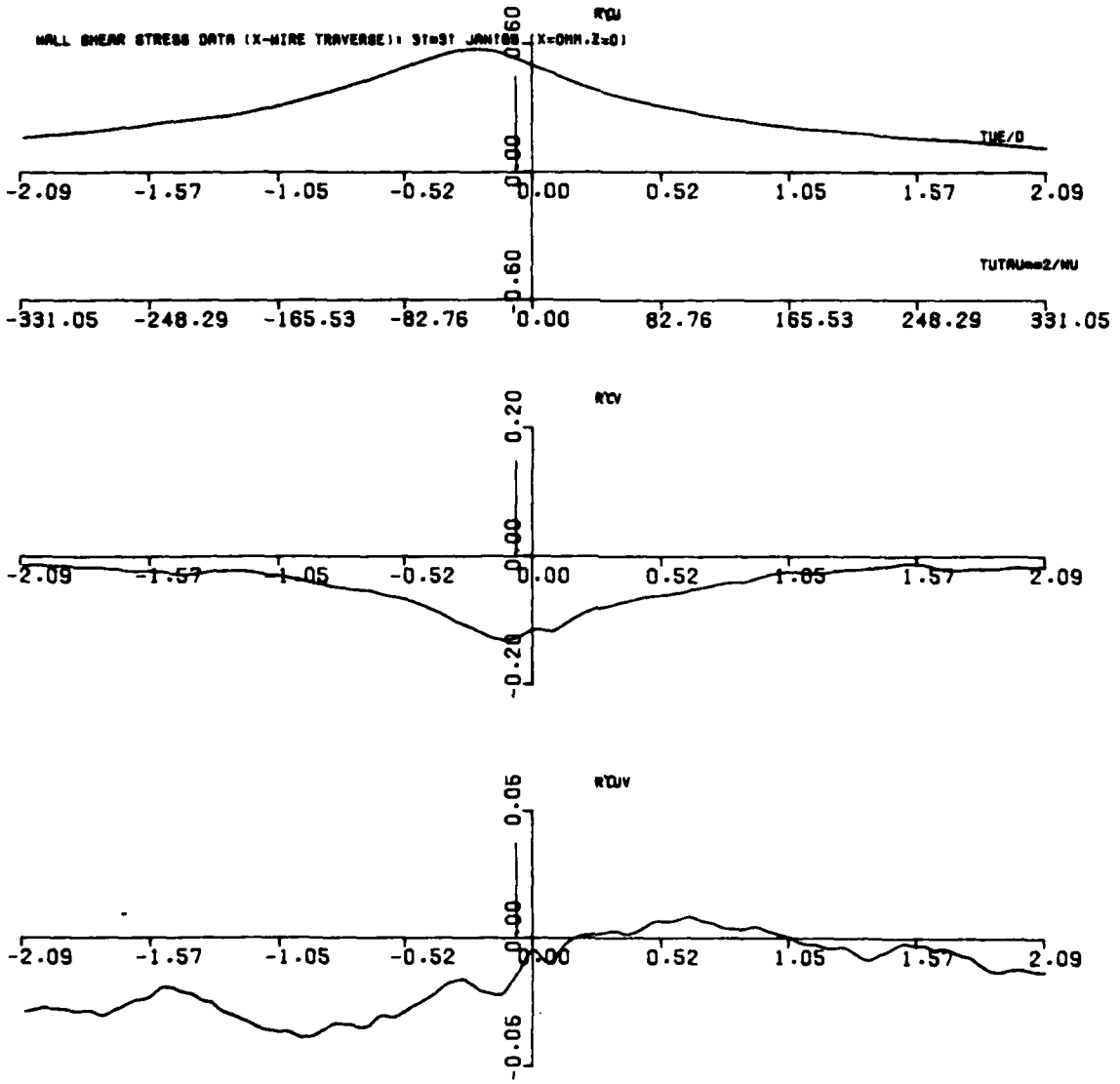

Fig.5 Wall shear stress-velocity space-time correlations.

5(a) Smooth, y/δ = .05

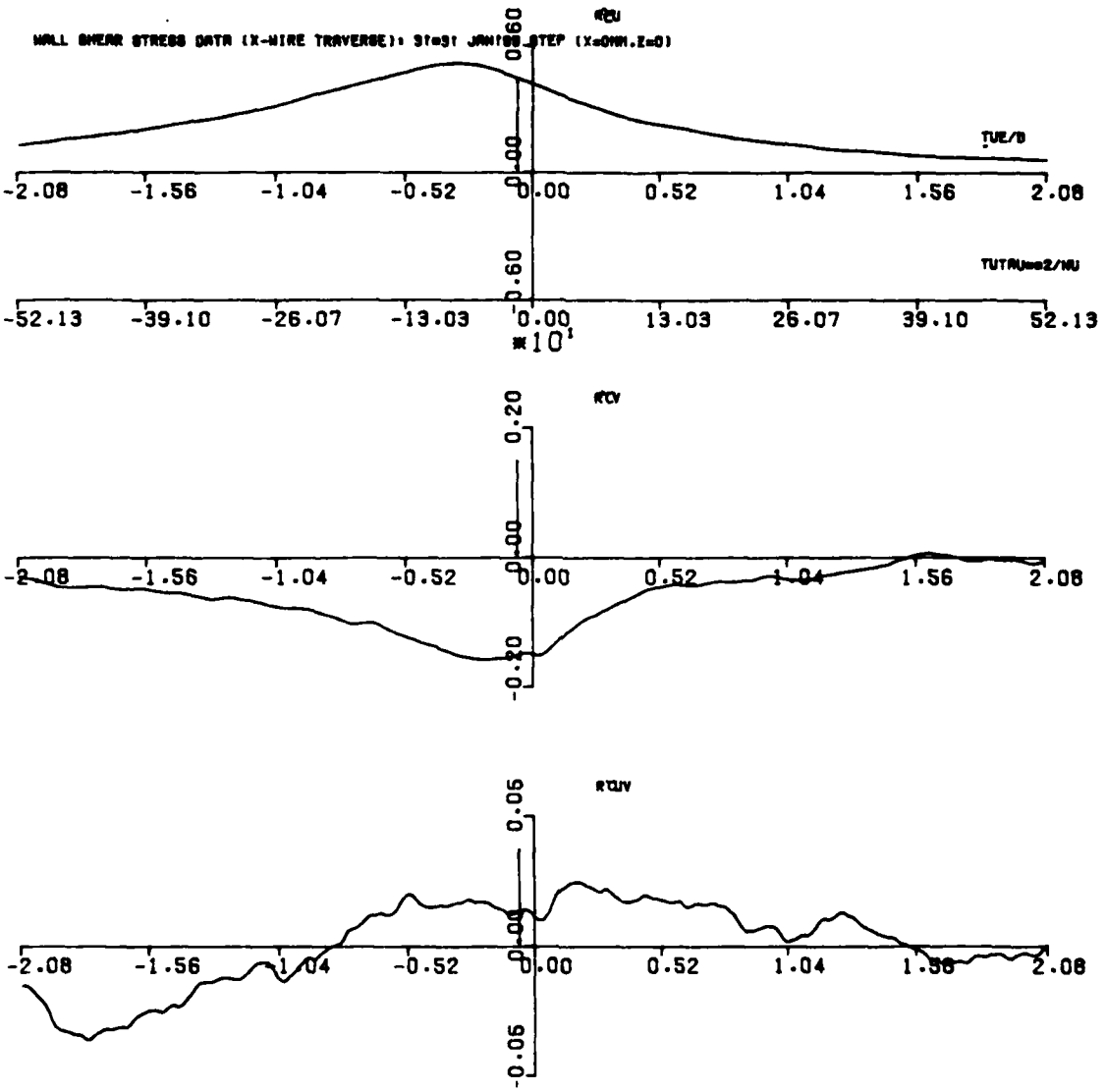

5(b) rough-to-smooth y/δ = .05

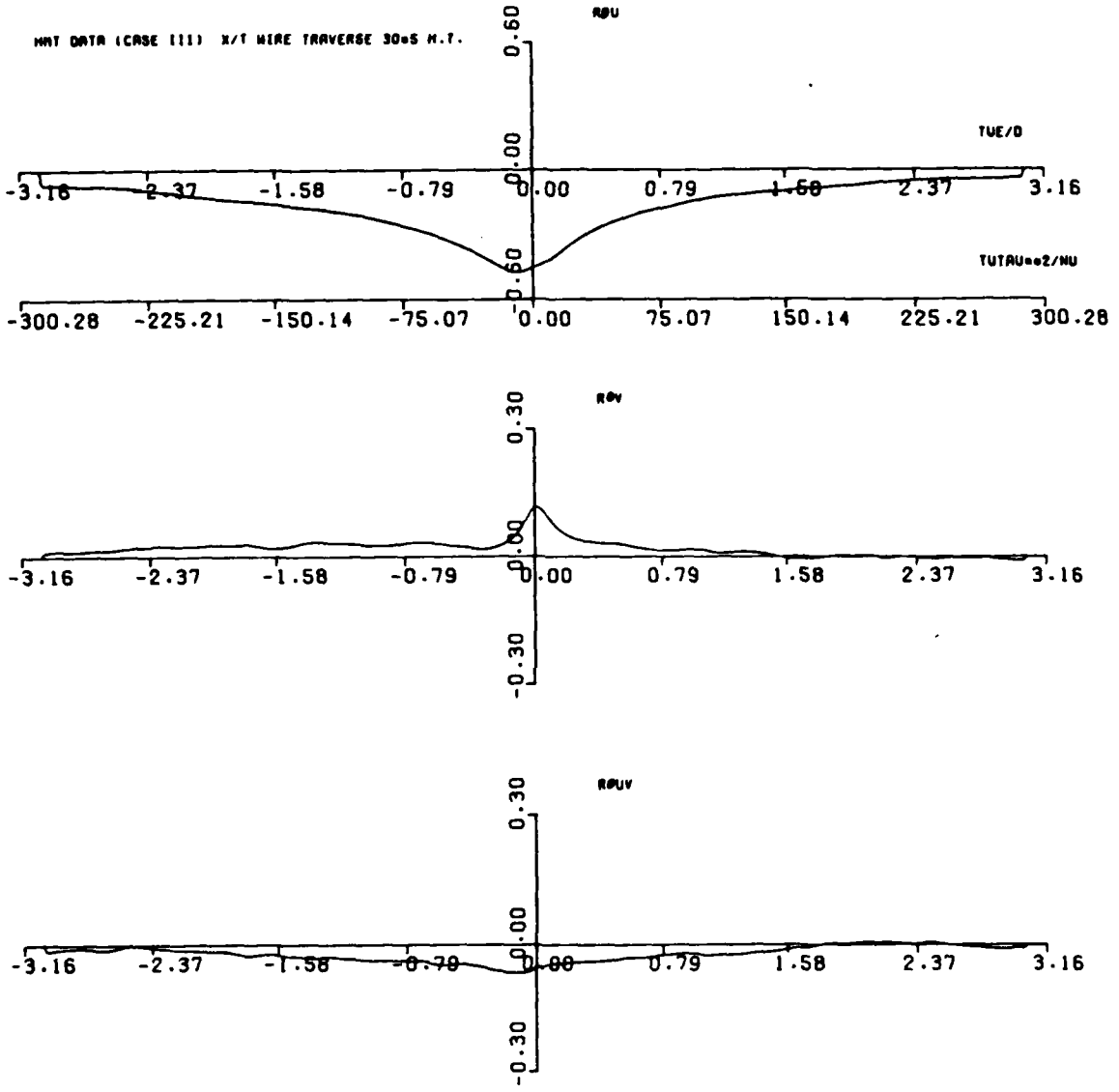

Fig.6 Temperature-velocity space-time correlations

6(a) smooth y/δ = .185

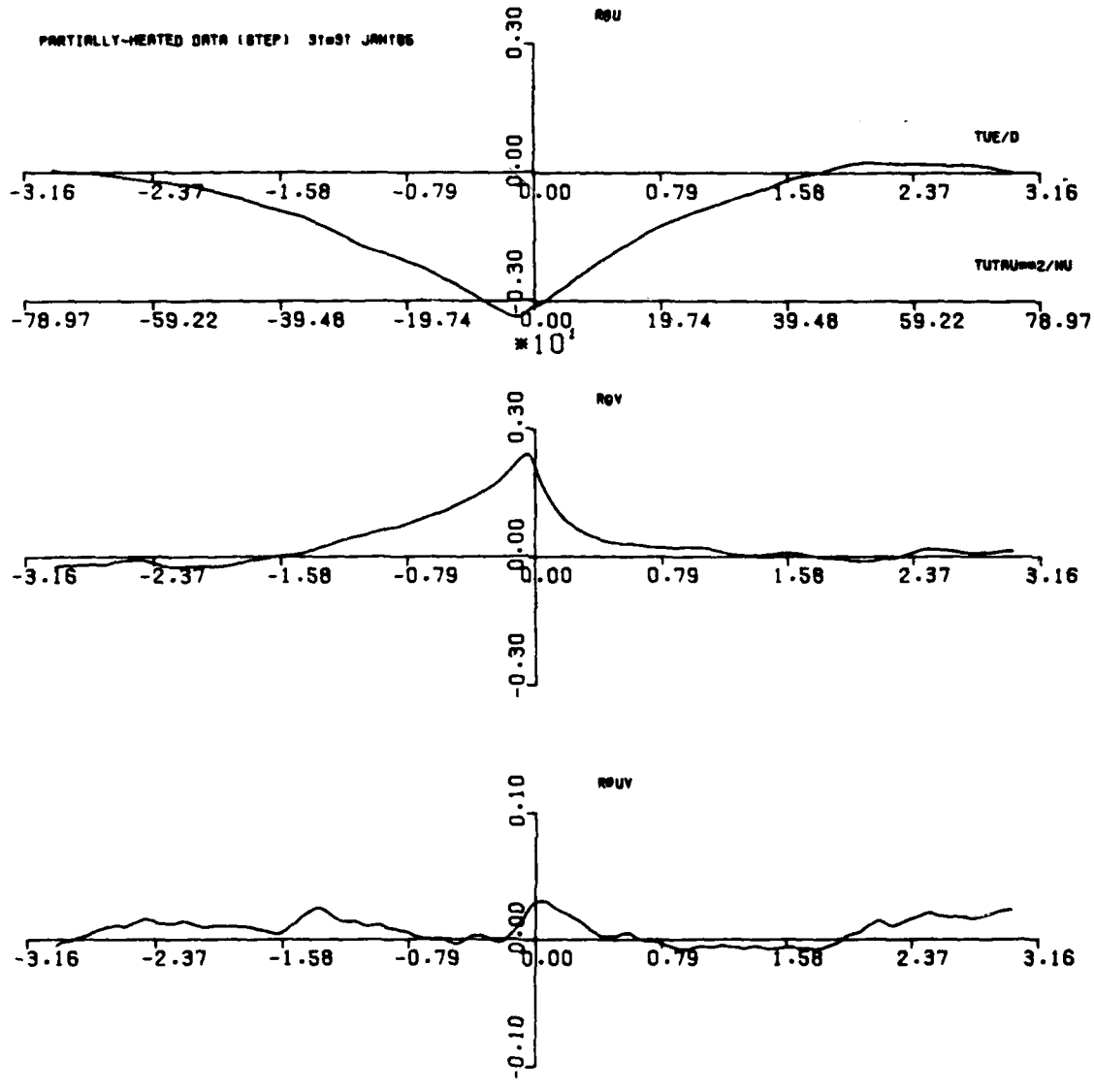

6(b) rough-to-smooth y/δ = 0.2

Section (C) November 1985 Periodic Report

Summary

The analysis of pressure- and velocity-fluctuation data outlined in the second periodic report, December 1984 - May 1985 (Section B, above) has been completed. Further work, suggested by the results obtained to date, is still in progress at no cost to the contract. Some analysis has also been done on relevant data obtained under one of the Principal Investigator's other contracts. This comprises measurements in a boundary layer slightly heated by a spanwise line source on the surface, so that eruptions ("bursts") from the wall region may be detected. These measurements have been used to help assess several conditional-sampling schemes used in the detection of eruptions. They also give a comparison for our own heated boundary layer measurements where the heat is introduced immediately following the rough-to-smooth change in surface roughness. (Figure 1 of Section A).

Scientific Work Statement

Results summarized in the December 1984 - May 1985 periodic report completed the conventional measurements in the "rough-to-smooth" surface flow, principally using space-time correlation techniques. Results for the remainder of the contract period, June 1985 - November 1985, have mainly involved the use of digital techniques for the selection of "interesting" periods of the various signals recorded in the rough-to-smooth flow and during the original smooth-surface experiment. The use of other workers' data has been important in this respect; heat introduced to a boundary layer near the wall has enabled 'hot' eruptions from the wall to be identified. The statistics from this data have helped us to assess the VITA (Variable Interval Time Averaging) sampling scheme. We have introduced some modifications so that statistics from an improved scheme, generated by sampling on the instantaneous uv-fluctuation, are

as nearly as possible independent of the sampling scheme. The same scheme is currently being used to generate statistics by sampling on the instantaneous spanwise component of vorticity, in collaboration with an SERC-supported research aimed at measuring the spanwise components of strain-rate and vorticity of the large-scale structure of a boundary layer.

The use of heat addition to the rough-to-smooth boundary layer has also been beneficial in elucidating our ideas concerning the outer, large-eddy, contribution to the near-wall motion. The heat is introduced immediately downstream of the transition so that eddies generated over the smooth part of the wall are nominally 'hot' while those generated over the rough wall are 'cold'. These data are compared with other investigators' work in the same tunnel, which used a smooth-walled unheated starting length but very nearly the same distance from the heater to the measurement station ("fetch"). A set of heated flow results and some of those from the VITA-based scheme are presented below.

Results

(a) Heated flow measurements

Figures 1-8 outline the behaviour of the heated boundary layer downstream of the rough-to-smooth change in roughness. Some comparisons are also made with the smooth-wall boundary layer which has very nearly the same heated streamwise fetch (about 1.5m) so that the thermal boundary layer has completely filled the hydrodynamic one at the measurement station in both instances. This may seem to conflict with the above statements that the "internal layer" of fluid which has returned to smooth-surface equilibrium occupies only the region $y/\delta < 0.2$, say. In fact it is known from the work of Antonia and Luxton (J. Fluid Mech. 53, 737, 1972) that the rough-to-smooth internal layer grows very slowly because of turbulent kinetic energy diffusion towards the wall, but there is no corresponding effect on the temperature-fluctuation field because the "rough wall" turbulence is initially cold. (This implies that large departures from Reynolds' analogy are likely to occur but we have not explored this point as yet).

Figure 1 shows the temperature intermittency (the fraction of time for which the flow at a given point was above the free stream temperature) in both cases. The lower values of in the rough-to-smooth configuration show how the penetration of the hot fluid by cold fluid has increased. Figures 3-5 show the $R_{u\theta}$, $R_{v\theta}$, and $R_{uv\theta}$ correlation coefficients respectively. The increased intensity of the outer layer in the rough-to-smooth configuration alters only the $R_{u\theta}$ correlation near the wall. This increase in $R_{u\theta}$ near the wall, without change in correlation involving v, is consistent with the usual ideas concerning "inactive motion" which is also responsible for a large increase in the R_{pu} correlation coefficient. Figure 6 shows the uv correlation non-dimensionalised by the friction velocity $u_\tau = \sqrt{(\tau w/\rho)}$ and the maximum temperature difference between the boundary layer and the free stream, T_{max}, is diferent in the two cases, while $R_{uv\theta}$ is nearly the same near the wall. ($R_{uv\theta}$ for the smooth wall is not shown.) This confirms that the inactive motion affects mainly the u-component, and is generated by motion which does not scale on u_τ.

The correlations of figures 2-5 include 'hot' and 'cold' contributions to the total: the sum of these contribution equals the total correlation. For example the "hot" contribution to R_{uv} is $\langle uv\rangle_{hot}/\sqrt{\overline{u^2}}.\sqrt{\overline{v^2}}$, where $\langle uv\rangle$ hot is the average value of uv over the hot zone: fluctuations are measured about the conventional mean velocity. As expected, most of the contributions to the R_{uv} correlation near the wall come from the "hot" zones, but that the cold contribution increases steadily further out in the boundary layer. The behaviour of the correlations such as $R_{uv\theta}$ which involve θ as a true variable (the fluctuation being measured with respect to the conventional-mean temperature and not the free-stream "cold" level) is interestingly different from the contributions to the corresponding velocity correlations, such as R_{uv}. In the outer part of the flow the "cold" contribution to R_{uv} has the opposite sign to the total correlation: this is simply because the temperature of the "cold" fluid is colder than the mean so that uv (which tends to be negative)

is multiplied by a negative Θ. The "cold" contribution to $R_{uv\theta}$ actually dominates near the wall, which suggests that cold, outer layer fluid plays an important part in the transport of shear stress in addition to eruptions of 'hot' fluid from the wall. Figures 7 and 8 show bulk convection velocities for the shear stress in the normal and streamwise directions respectively. The hot eruptions from near the wall are suppressed by the intensity of the outer layer motion while the convection of shear stress towards the wall is double that of the smooth wall boundary layer. The streamwise bulk convection velocity of uv shows a similar effect: the streamwise convection of shear stress by the cold fluid near the wall is approximately doubled and that by hot fluid severely attenuated - by a factor of ten at $y/\delta=0.3$.

(b) Shear-stress-conditioned statistics

The remaining figures show statistics generated by averaging over selected events only. The VITA criterion has been amended so that the events detected are as independent of threshold as possible. Particular care has been taken so that the lengths of these events are not criterion-dependent; once VITA has detected an event, the beginning and end of the event are located by a simple level criterion that is non-dimensional.

Specifically, events must satisfy:

$$\text{var}(uv) > \text{VITH}\left(\overline{u^2}.\ \overline{v^2}\right)^{1/2}$$

and

$$|uv| > \text{TH}\left(\overline{u^2}.\ \overline{v^2}\right)^{1/2}$$

where var(F) denotes the average of a function F(t) over a time $0.06\ /U_e$, and the dimensionless thresholds are VITH = 0.2 and TH = 0.46. The value of TH is just above the expected value of the shear correlation coefficient, so our extra "level" criterion is almost equivalent to requiring $|uv| > |\overline{uv}|$.

Figures 9-14 show event durations and corresponding streamwise lengths (calculated using the event-averaged velocity as the convection velocity). Events are subdivided into those moving towards, and those moving away from, the wall. The intermittency of these events is constant over much of the boundary layer, typically 0.2. Event-averaged shear correlation coefficients are typically 0.8 for all values of y/δ: third-order correlation coefficients are also near unity. These results suggest that the events we detect are well organised and extremely efficient in mixing turbulence. Yet the durations and lengths of these events do not tally with the usual inner layer arguments, which would require all length scales of the shear-stress producing part of the turbulence to be proportional to y. In fact the variation with y is disconcertingly close to the $y^{1/4}$ variation of the Kolmogorov viscous scale η. The most obvious explanation is that the VITA algorithm ought to use an integration time proportional to y/U, but (i) this assumes the truth of the inner layer scaling we are trying to investigate;(ii) previous - perhaps less demanding - workers have all used VITA integration times independent of y. The actual time chosen corresponds to a streamwise distance of about 0.1δ (the velocity in the log-law region being roughly $0.6U_e$) which seems a reasonable choice for the larger events in the region $0.05<y/\delta<0.2$. These results require further thought and investigation. It is important to establish the connection, if any, between these events and the universality of the logarithmic region. It may be that 'agglomerations' of these events give rise to the usual 'law of the wall' scalings. Indeed, also shown on figure 10 are the lengths calculated from the abscissae of R_{puv} space-time correlations (figure 3 of Section B). A negative event notionally corresponds to a burst of fluid away from the wall for which the R_{puv} correlation is positive. These lengths increase as the usual 'mixing length' arguments would suggest. Figures 15 and 16 show the total R_{puv} correlation coefficients together with contributions to the total by positive and negative events. These indicate that the events detected are at least primarily responsible for the shape of the total R_{puv} correlation near the wall.

Further work

Further analysis is envisaged to answer the questions raised above. This involves the use of the sampling scheme with the spanwise component of vorticity and the investigation of events in their relation to the 'law of the wall'. Convection velocities of pressure fluctuations concerned with these events will also be deduced.

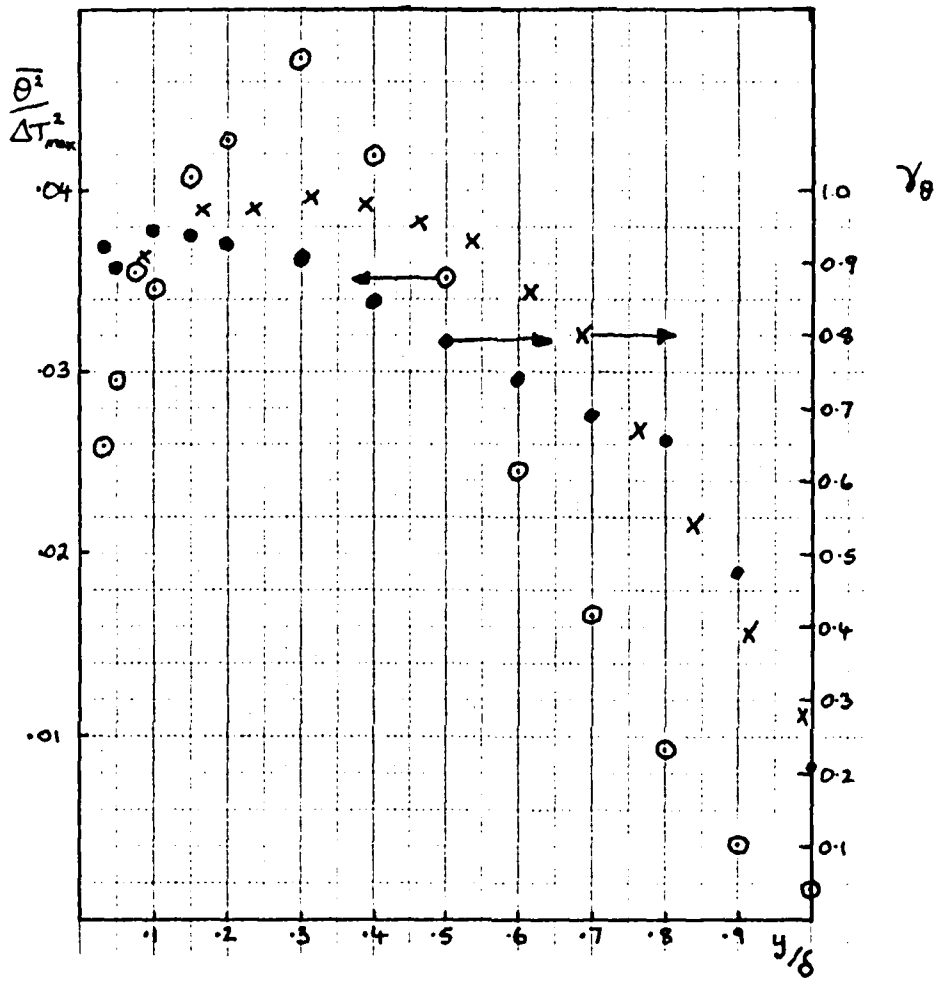

Figure 1 Mean-square temperature fluctuations and temperature intermittency γ_θ: ●, ROUGH-TO-SMOOTH; X, SMOOTH.

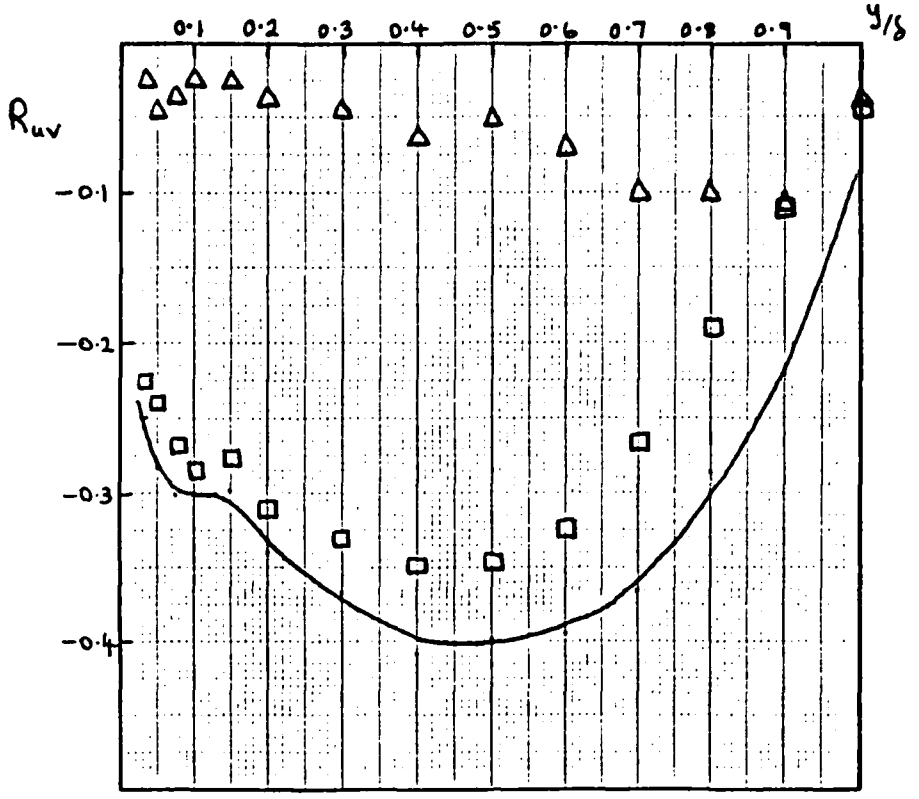

Figure 2 Rough-to-smooth R_{uv} correlation coefficient: — total; □,'hot' contribution (γR_{uv}); Δ, 'cold' contribution ($(1-\gamma)R_{uv}$).

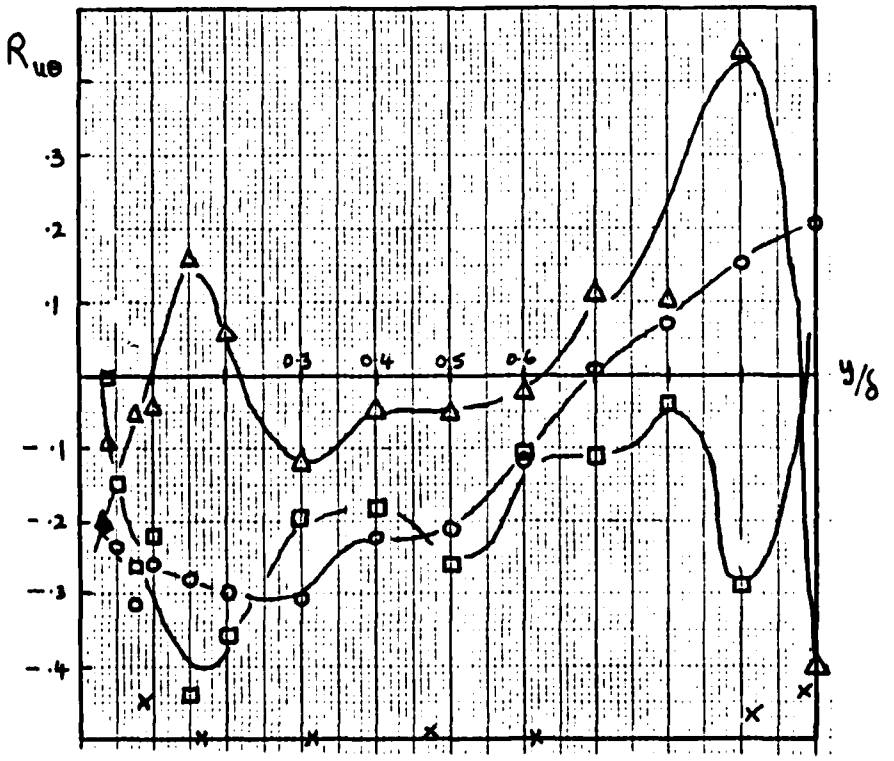

Figure 3 $R_{u\theta}$ correlation coefficient: O, total (rough-to-smooth); x, total (smooth). Contributions (rough-to-smooth): □, 'hot'; Δ, 'cold'.

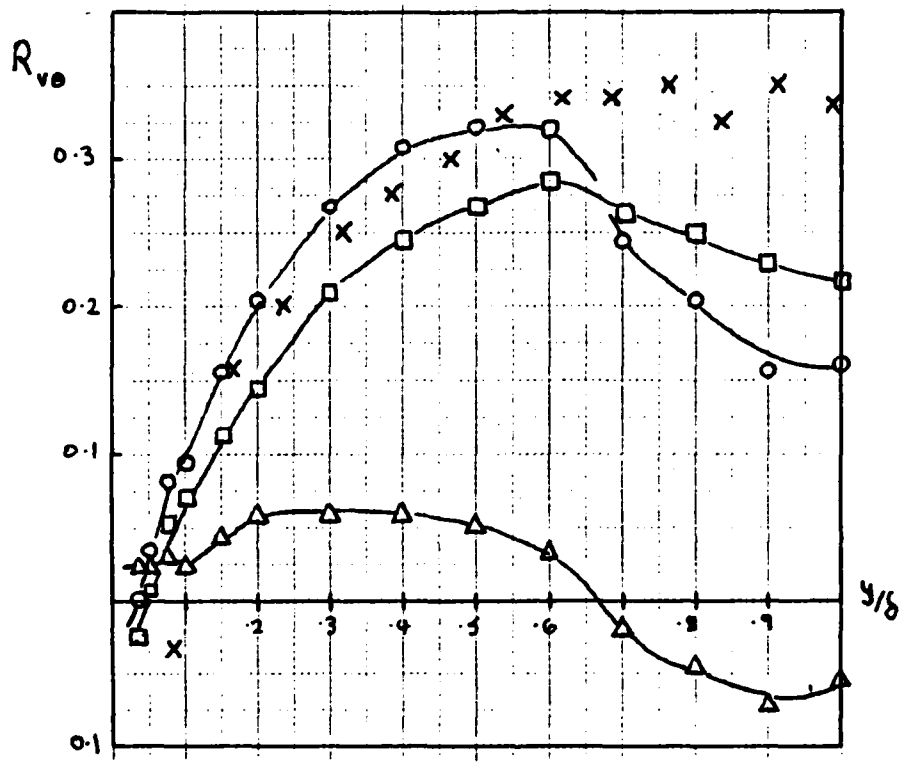

Figure 4 $R_{v\theta}$ correlation coefficient: symbols as in figure 2.

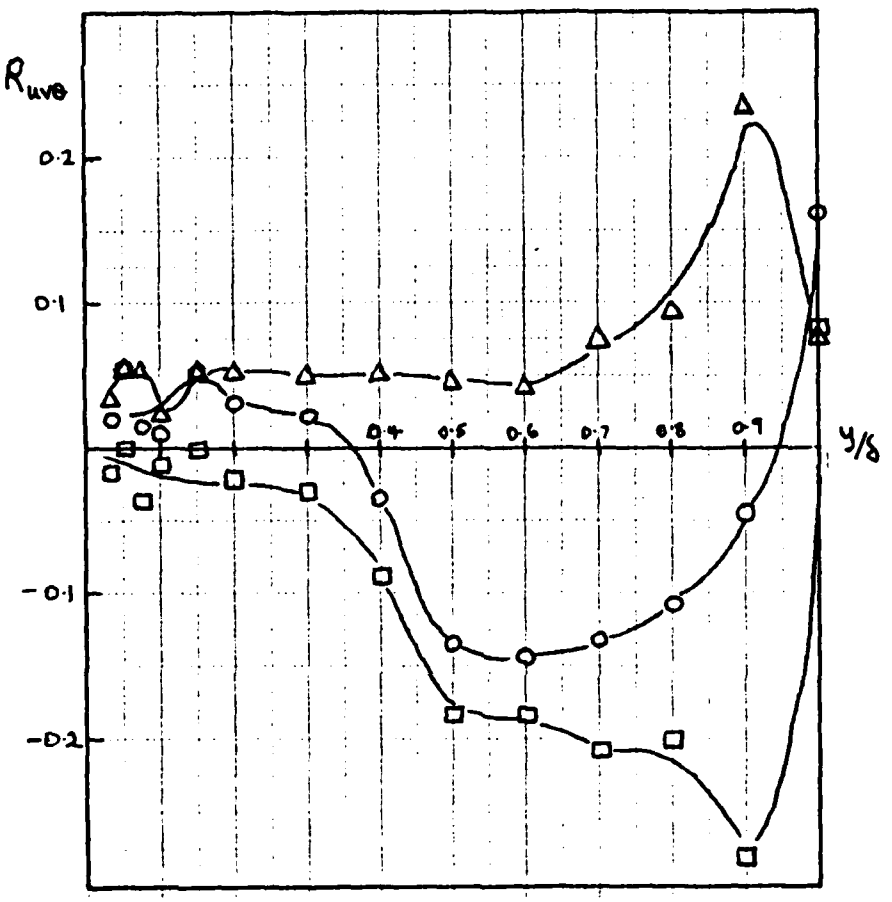

Figure 5 $R_{uv\theta}$ correlation coefficient: symbols as in figure 2.

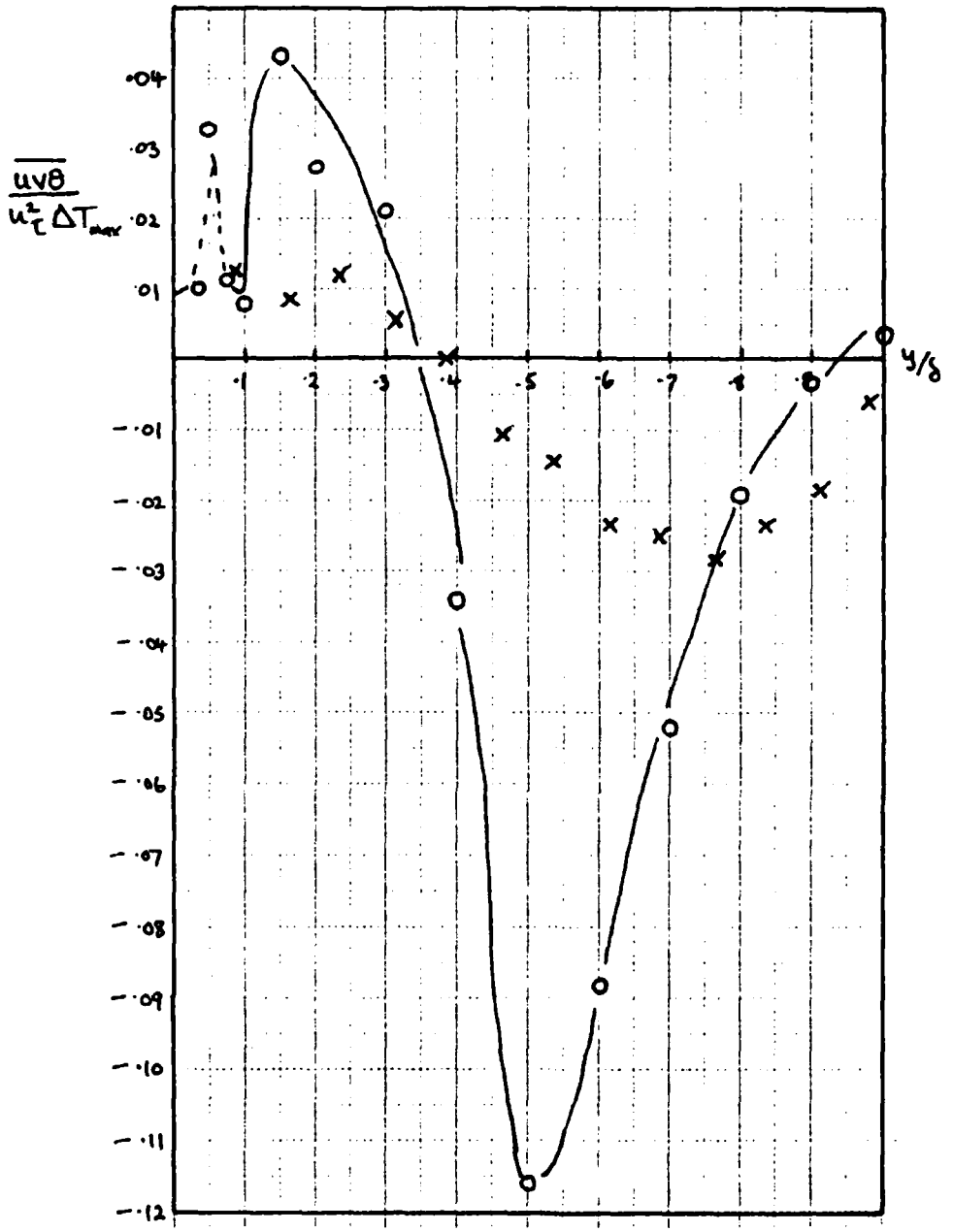

Figure 6 $\overline{uv\theta}/u_\tau^2 \Delta T_{max}$: symbols as in figure 2

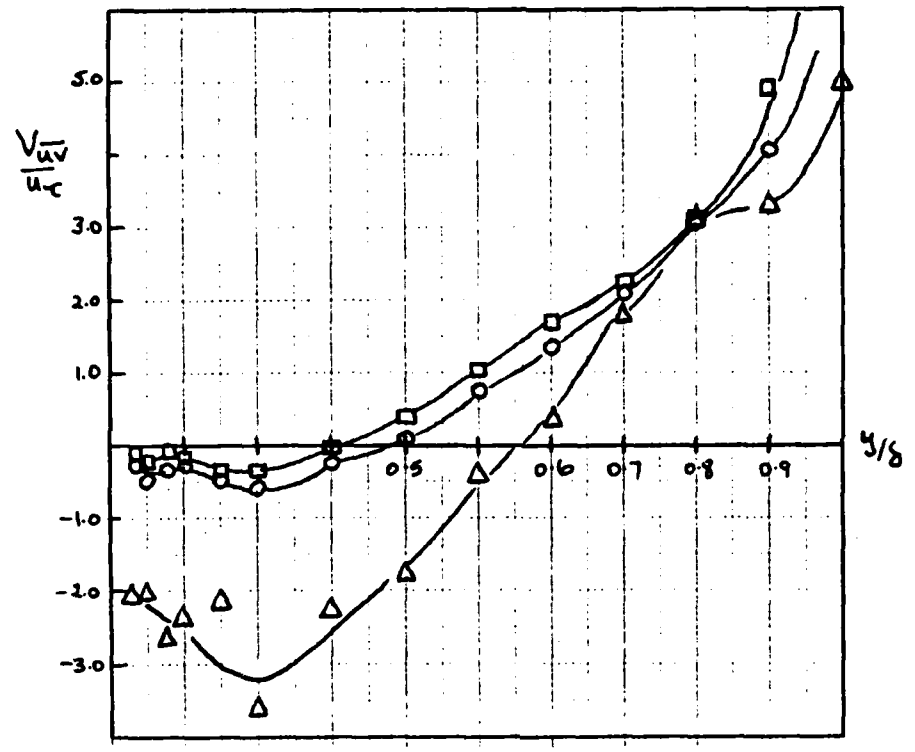

Figure 7 Convection velocity $V_{\overline{uv}}/u_\tau = \dfrac{\overline{uv^2}}{\overline{uv}.u_\tau}$: 0, total; □, 'hot' velocity; Δ, 'cold' velocity.

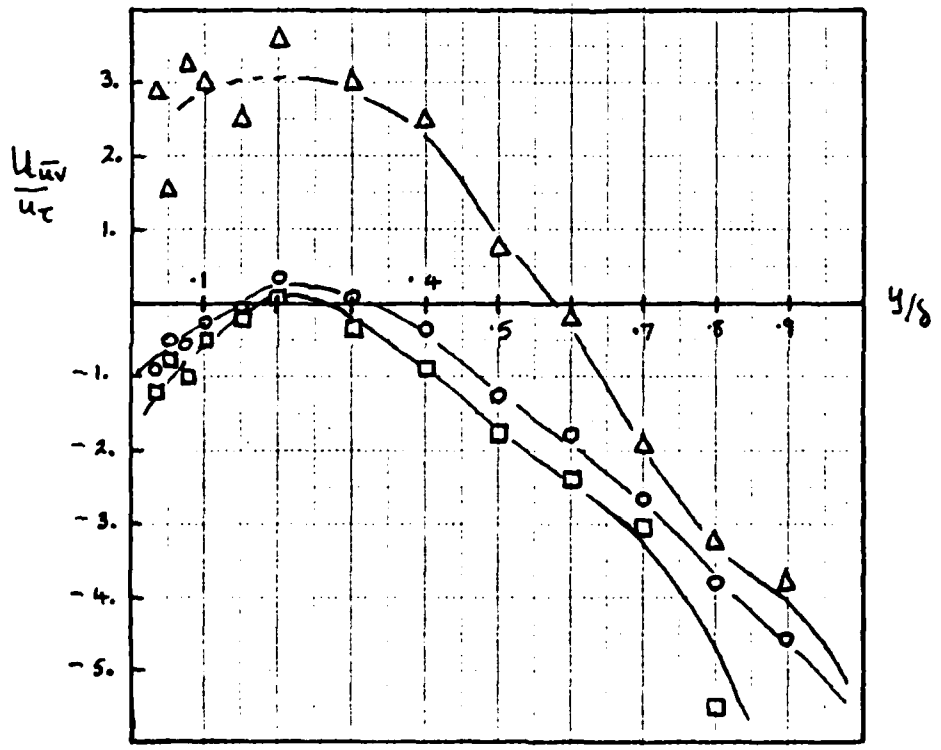

Figure 8 Convection velocity $U_{\overline{uv}}/u_\tau = \dfrac{\overline{u^2v}}{\overline{uv}\ u_\tau}$: symbols as in figure 7.

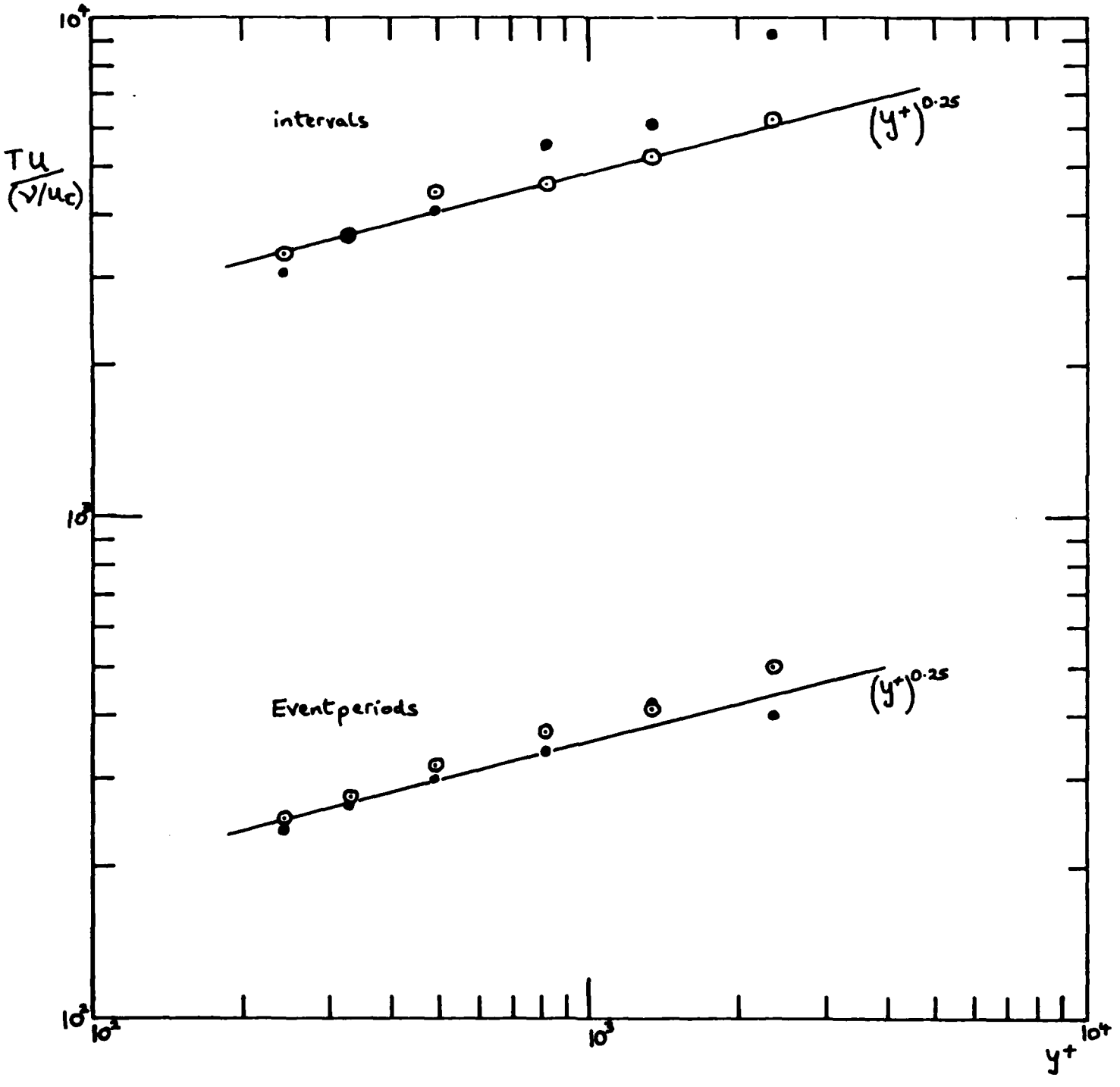

Figure 9 Period of events and interval as average time between events: •, + events; θ - events. (Smooth wall).

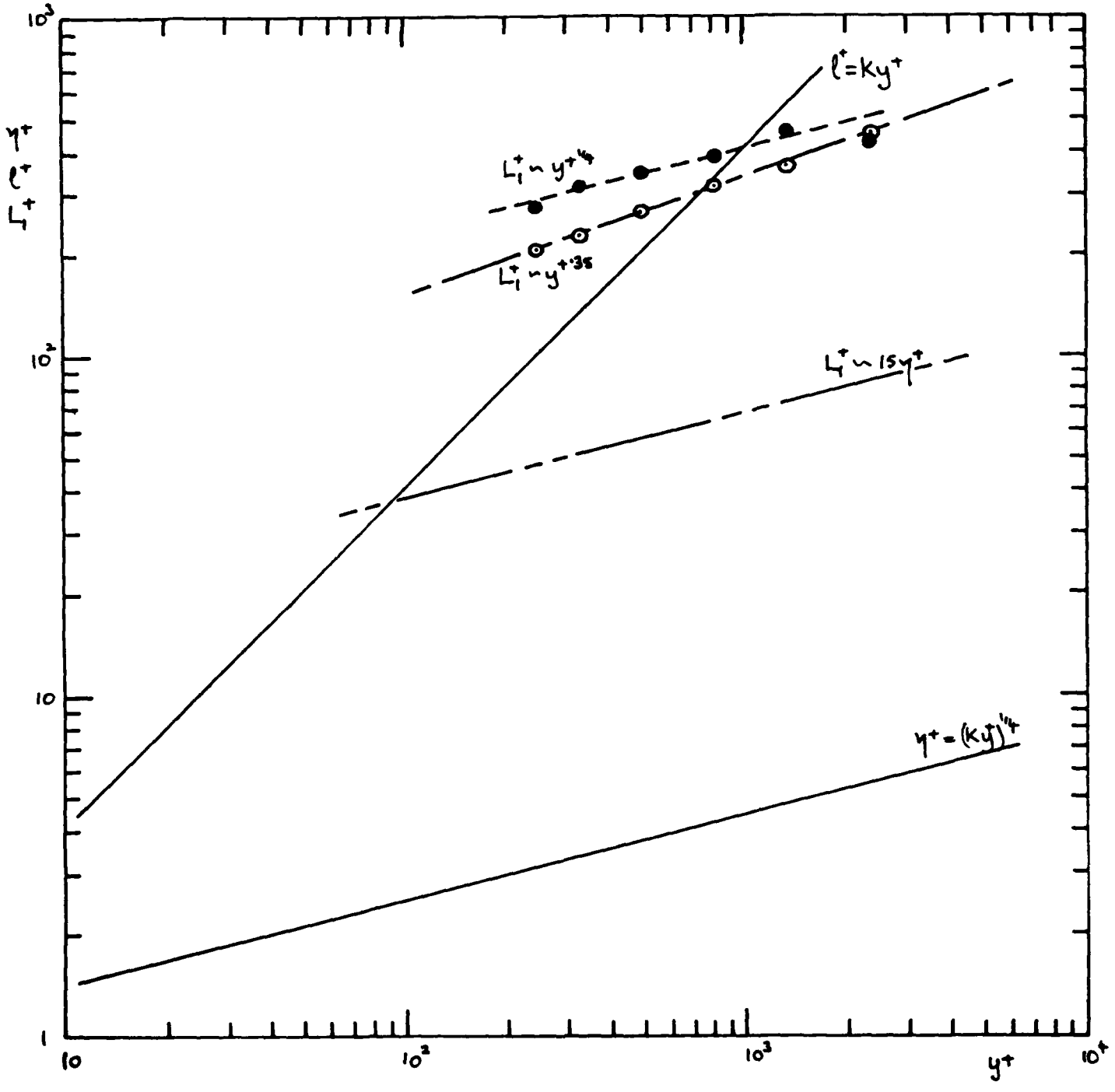

Figure 10 First moment (average) of p.d.f. of event lengths (smooth wall). Symbols as in figure 9.

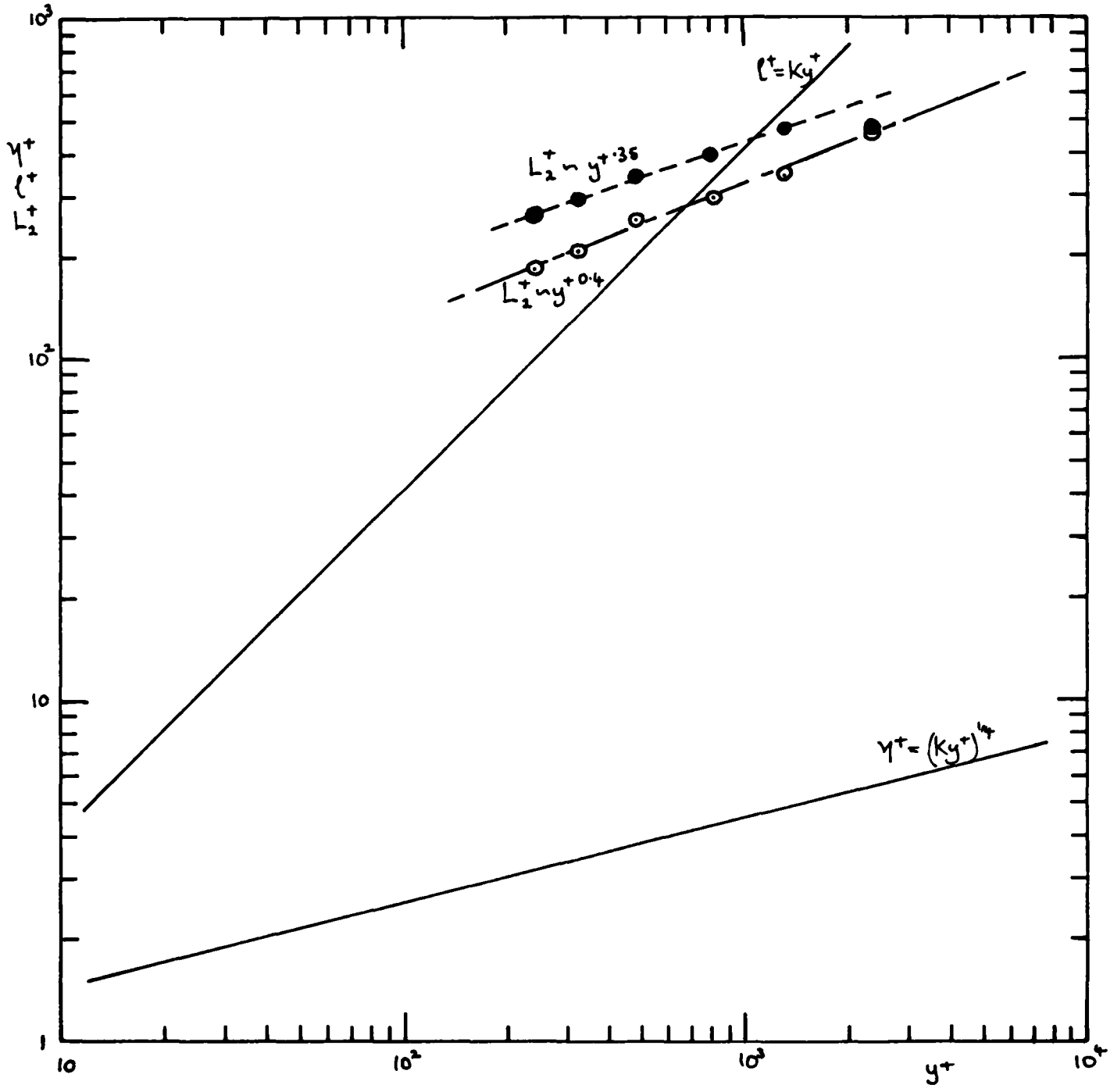

Figure 11 Second moment (standard deviation) of p.d.f. of event lengths (smooth wall). Symbols as in figure 9.

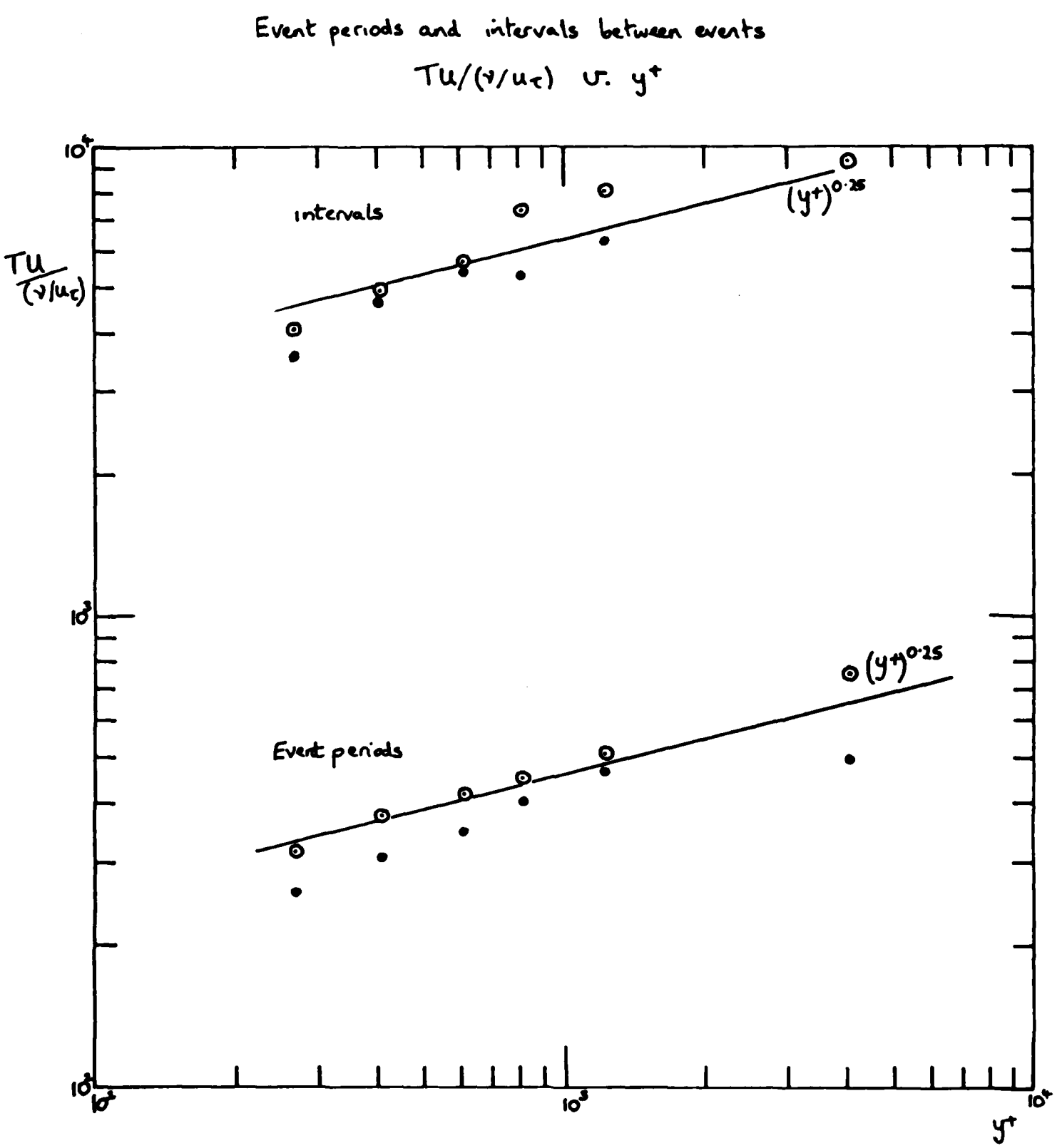

Figure 12 Period of events and intervals as average time between events (rough-to-smooth): symbols as in figure 9.

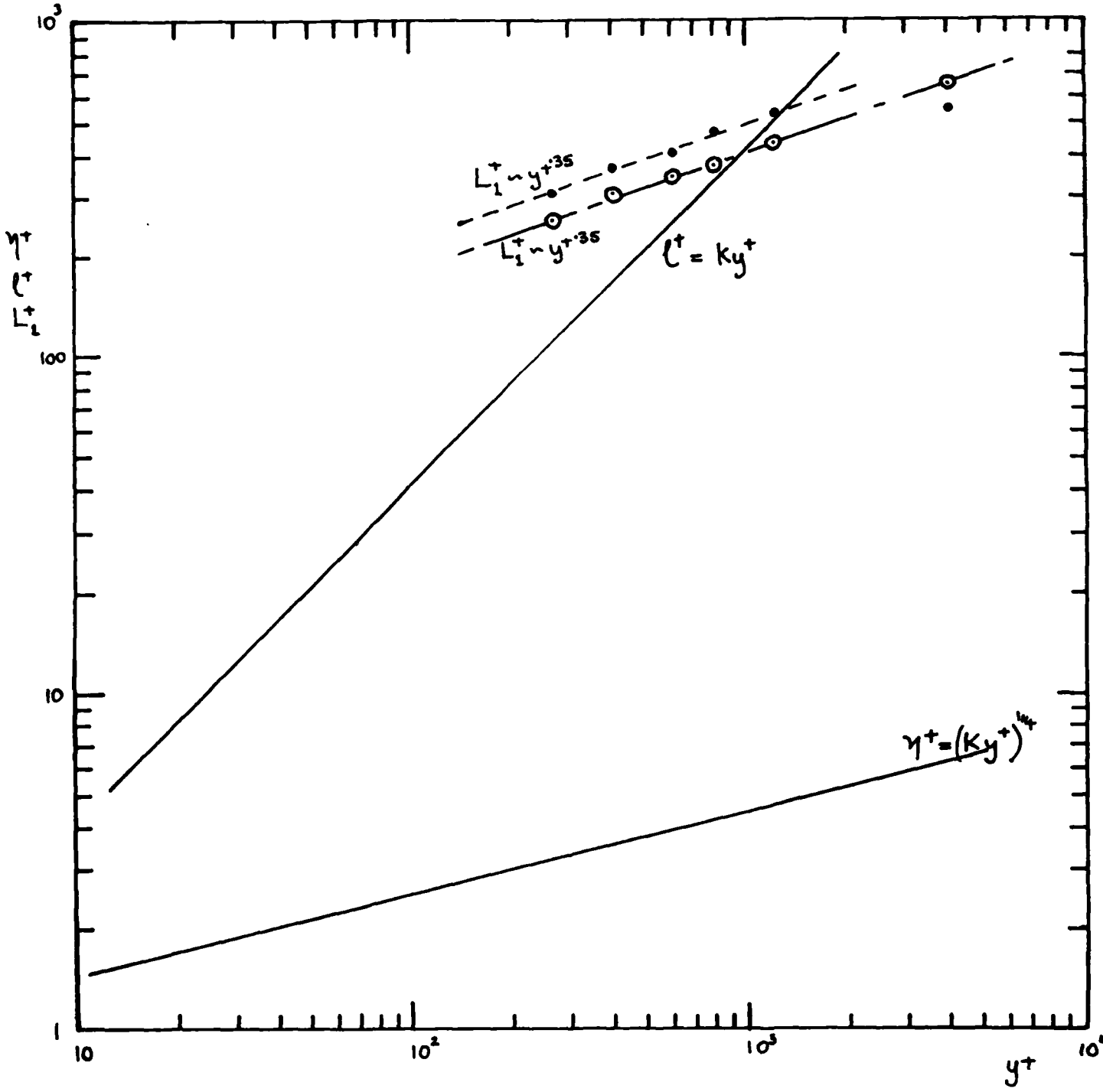

Figure 13 First moment of p.d.f. of event lengths (rough-to-smooth). Symbols as in figure 9.

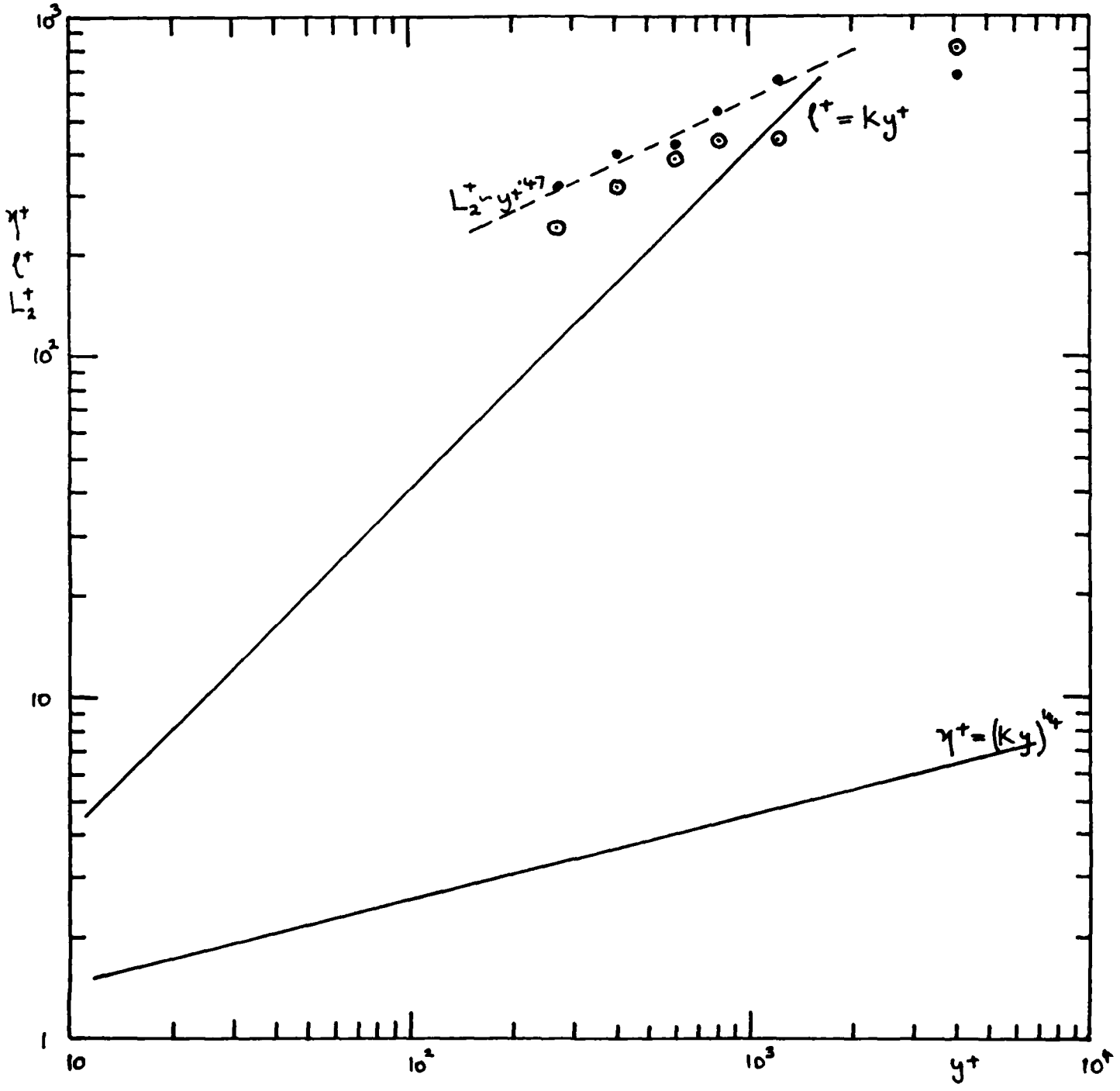

Figure 14 Second moment of p.d.f. of event lengths (rough-to-smooth). Symbols as in figure 9.

Figure 15 Space-time correlation coefficient R_{puv} (shear stress - wall pressure): —— total; - - - -, $\gamma^- R_{puv}^-$; - —— - , $\gamma^+ R_{puv}^+$. Smooth wall, $y/\delta \approx .051$.

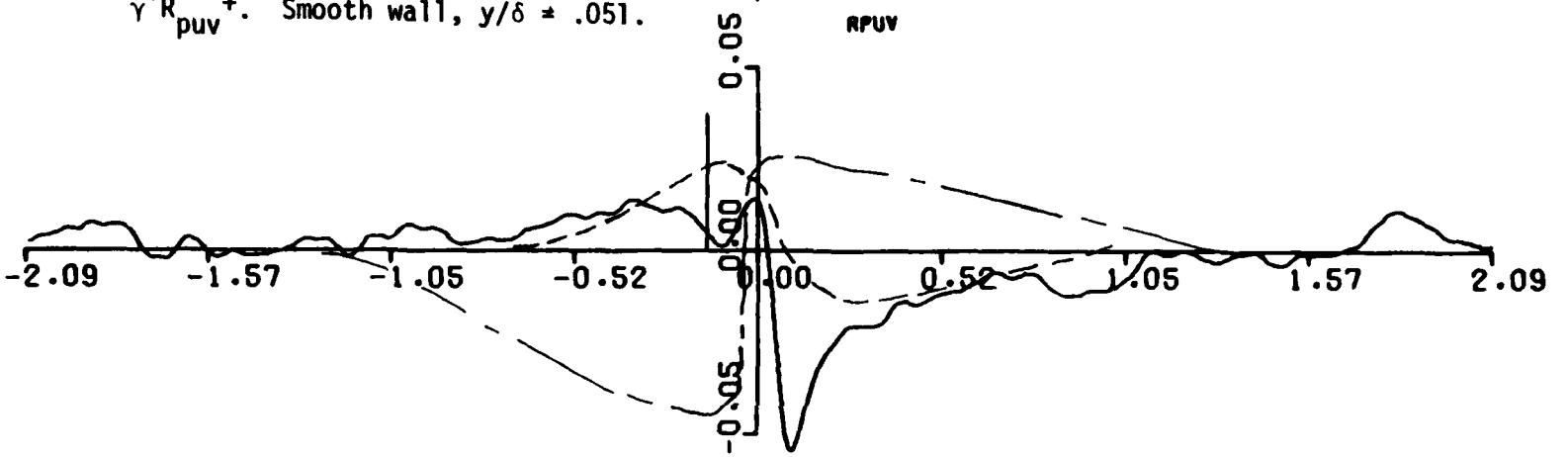

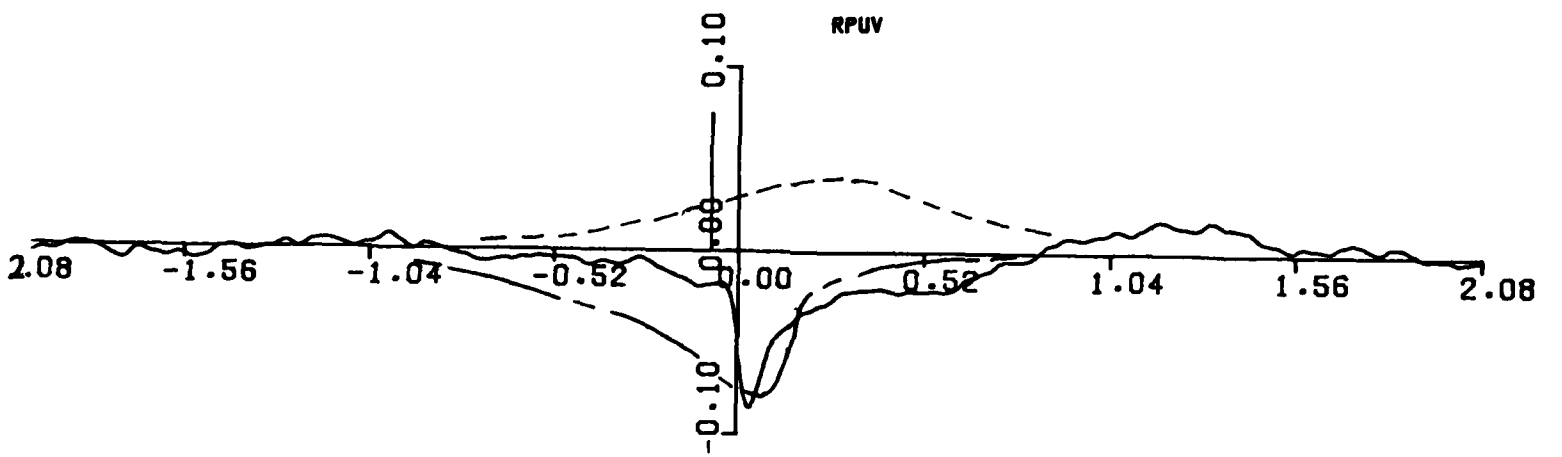

Figure 16 Space-time correlation coefficient R_{puv}: Rough-to-smooth $y/\delta = .033$.

END

FILMED

DTIC

6-86